JACS
JOURNAL OF THE AMERICAN CHEMICAL SOCIETY

ARTICLE

pubs.acs.org/JACS

Thorium Oxo and Sulfido Metallocenes: Synthesis, Structure, Reactivity, and Computational Studies

Wenshan Ren,[†] Guofu Zi,*[,†] De-Cai Fang,*[,†] and Marc D. Walter*[,‡]

[†]Department of Chemistry, Beijing Normal University, Beijing 100875, China

[‡]Institut für Anorganische und Analytische Chemie, Technische Universität Braunschweig, Hagenring 30, 38106 Braunschweig, Germany

Supporting Information

ABSTRACT: The synthesis, structure, and reactivity of thorium oxo and sulfido metallocenes have been comprehensively studied. Heating of an equimolar mixture of the dimethyl metallocene $[\eta^5\text{-}1,2,4\text{-}(Me_3C)_3C_5H_2]_2ThMe_2$ (**2**) and the bis-amide metallocene $[\eta^5\text{-}1,2,4\text{-}(Me_3C)_3C_5H_2]_2Th(NH\text{-}p\text{-}tolyl)_2$ (**3**) in refluxing toluene results in the base-free imido thorium metallocene, $[\eta^5\text{-}1,2,4\text{-}(Me_3C)_3C_5H_2]_2Th{=}N(p\text{-}tolyl)$ (**4**), which is a useful precursor for the preparation of oxo and sulfido thorium metallocenes $[\eta^5\text{-}1,2,4\text{-}(Me_3C)_3C_5H_2]_2Th{=}E$ (E = O (**5**) and S (**15**)) by cycloaddition−elimination reaction with $Ph_2C{=}E$ (E = O, S) or CS_2. The oxo metallocene **5** acts as a nucleophile toward alkylsilyl halides, while sulfido metallocene **15** does not. The oxo metallocene **5** and sulfido metallocene **15** undergo a [2 + 2] cycloaddition reaction with Ph_2CO, CS_2, or Ph_2CS, but they show no reactivity with alkynes. Density functional theory (DFT) studies provide insights into the subtle interplay between steric and electronic effects and rationalize the experimentally observed reactivity patterns. A comparison between Th, U, and group 4 elements shows that Th^{4+} behaves more like an actinide than a transition metal.

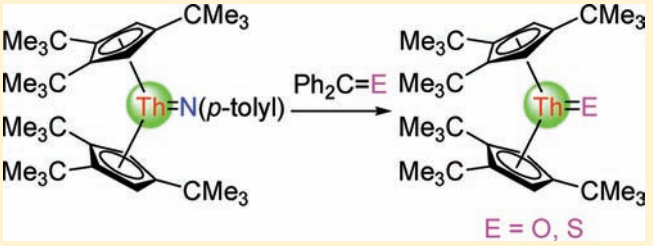

1. INTRODUCTION

The organoactinide complexes containing terminal metal−ligand multiple bonds have received widespread attention over the past two decades due to their unique structural properties and their potential applications in group transfer and catalysis.[1] Among these, oxo and sulfido organoactinide complexes are of particular interest,[1−4] because these functionalities are ubiquitous in actinide chemistry, as shown by the prevalence of binary oxides and sulfides in the solid state.[5] In this context, well-defined molecular structures will advance our understanding of the bonding and reactivity of An=O and An=S functional groups and help to uncover novel transformations that may be used in industrial environments. For example, the interaction between solid U_3O_8 and chlorocarbons results in complete destruction of the latter to CO_x and HCl.[6] This unusual and potentially useful reaction probably occurs at U−O functional groups on the surface U−O. While many oxo organouranium complexes have been prepared, only a few of them exhibit significant reactivity, and many studies have focused on their structural characterizations.[2,3] However, the reaction of alkylhalides with the model complex $[\eta^5\text{-}1,2,4\text{-}(Me_3C)_3C_5H_2]_2U{=}O$ provides information on the nature of the U=O bond on a molecular level.[3e] In contrast to oxo organouranium chemistry, to the best of our knowledge, no examples of other actinide metal oxo organometallic complexes have been reported. Furthermore, only a few actinide complexes contain purely inorganic chalcogenide ligands and only one example of a terminal actinide sulfido complex, uranium sulfido complex $[Na(18\text{-crown-}6)][(\eta^5\text{-}Me_5C_5)_2U(S)(SCMe_3)]$, has been structurally authenticated.[4] Thus, the development of novel actinide oxo and sulfido complexes remains an interesting and challenging synthetic target. In the course of our studies of actinide complexes, we are interested in thorium metallocenes with Th=E (O and S) double bonds. This research is motivated by the fact that ThO_2 has been used as a catalyst for various chemical transformations. While it can serve in some reactions as a support for other catalysts, a catalytic activity of ThO_2 itself cannot be excluded in these cases. Most notable is the activity of ThO_2 in Fischer−Tropsch synthesis, hydrogenation and dehydrogenation, and oxidation reactions.[7] In addition, thorium has a ground-state electron configuration of $7s^26d^2$, which suggests that it might exhibit reactivity similar to group 4 elements, such as Ti, Zr, and Hf, for which the corresponding metallocenes with M=E (E = O and S) have been prepared.[8] This comparison also addresses the question whether the Th^{4+} should be considered as an actinide or as a transition metal and whether f-orbitals contribute to the bonding in thorium organometallics.[8−10] Although thorium oxo and sulfido metallocenes have not been described so far, two examples of oxo and one example of sulfido uranium(IV) metallocenes have been structurally authenticated.[3d,e,4] It has

Received: June 8, 2011
Published: July 27, 2011

dx.doi.org/10.1021/ja205280k | J. Am. Chem. Soc. 2011, 133, 13183–13196

Scheme 1

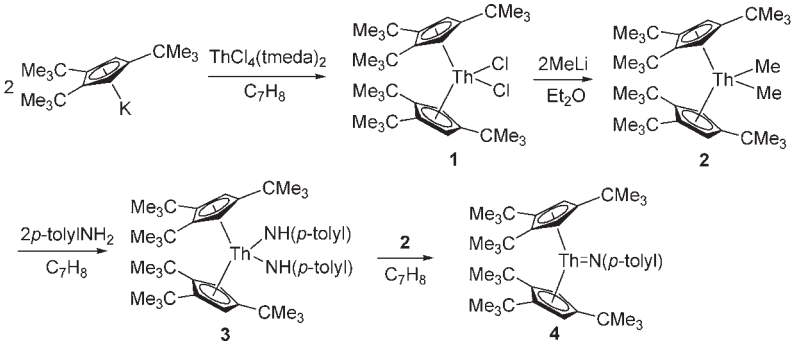

been noted that uranium(IV) oxo or sulfido metallocene formation is especially sensitive to steric effects imposed by the cyclopentadienyl ligand. The formation of dimers with bridging oxo or sulfido groups is often observed due to the potent basicity of these groups.[3e,4] For example, the ligand 1,3-$(Me_3C)_2C_5H_3$ yields the oxo-dimer $\{[\eta^5\text{-}1,3\text{-}(Me_3C)_2C_5H_3]_2U\}_2(\mu\text{-}O)_2$,[11] while the sterically very encumbered cyclopentadienyl ligand 1,2,4-$(Me_3C)_3C_5H_2$ can efficiently stabilize the base-free uranium oxo metallocene $[\eta^5\text{-}1,2,4\text{-}(Me_3C)_3C_5H_2]_2U{=}O$ (monomeric in gas phase).[3e] Encouraged by the attractive feature of this bulky ligand, we have recently started exploring the 1,2,4-$(Me_3C)_3C_5H_2$ ligand in thorium chemistry. We have found that the 1,2,4-$(Me_3C)_3C_5H_2$ ligand stabilizes the base-free thorium imido metallocene, $[\eta^5\text{-}1,2,4\text{-}(Me_3C)_3C_5H_2]_2Th{=}N(p\text{-tolyl})$ (**4**). Herein, we report the synthesis of the imido metallocene **4**, its use in the preparation of oxo and sulfido metallocenes, $[\eta^5\text{-}1,2,4\text{-}(Me_3C)_3C_5H_2]_2Th{=}E$ (E = O (**5**) and S (**15**)), and their reactivity. In addition, the differences and similarities between the uranium(IV), thorium(IV), and group 4 metallocenes will be addressed in this Article.

2. RESULTS AND DISCUSSION

2.1. Imido Metallocene $[\eta^5\text{-}1,2,4\text{-}(Me_3C)_3C_5H_2]_2Th{=}N(p\text{-tolyl})$. Treatment of $ThCl_4(tmeda)_2$ with 2 equiv of $[1,2,4\text{-}(Me_3C)_3C_5H_2]K$ in boiling toluene gives the dichloro metallocene, $[\eta^5\text{-}1,2,4\text{-}(Me_3C)_3C_5H_2]_2ThCl_2$ (**1**), in 85% yield. Salt metathesis between **1** and 2 equiv of MeLi in diethyl ether affords the dimethyl metallocene, $[\eta^5\text{-}1,2,4\text{-}(Me_3C)_3C_5H_2]_2ThMe_2$ (**2**), in 79% yield. Subsequent reaction of **2** with 2 equiv of *p*-toluidine in toluene gives the bis-amido metallocene, $[\eta^5\text{-}1,2,4\text{-}(Me_3C)_3C_5H_2]_2Th(NH\text{-}p\text{-tolyl})_2$ (**3**), in 90% yield. Finally, heating of an equimolar mixture of **2** and **3** in refluxing toluene gives the desired base-free imido thorium metallocene, $[\eta^5\text{-}1,2,4\text{-}(Me_3C)_3C_5H_2]_2Th{=}N(p\text{-tolyl})$ (**4**), in 85% yield (Scheme 1). Imido **4** is soluble in and readily recrystallized from toluene solution, but only slightly soluble in *n*-hexane. The ^1H and $^{13}C\{^1H\}$ NMR spectra indicate that it is symmetrical on the NMR time scale, which is consistent with its C_{2v}-symmetric structure. The ^1H NMR spectrum of **3** shows that the singlet of the N*H* groups at δ 5.07 ppm disappears upon treatment of **3** with **2**, and the ratio of the Cp-ligand and *p*-tolyl group changes to 2:1. In addition, the infrared spectrum shows the disappearance of the characteristic N−H absorption at 3254 cm^{-1} and therefore supports the formation of **4**.

Scheme 2

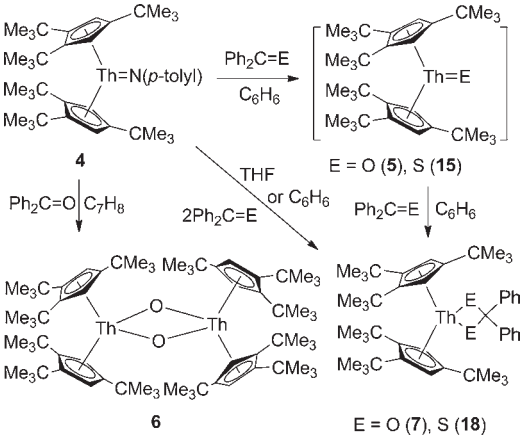

2.2. Thorium Oxo Metallocenes. It has been shown that the reaction of uranium *p*-tolylimido metallocene, $[\eta^5\text{-}1,2,4\text{-}(Me_3C)_3C_5H_2]_2U{=}N(p\text{-tolyl})$, with 1 or 2 equiv of Ph_2CO gives the oxo metallocene, $[\eta^5\text{-}1,2,4\text{-}(Me_3C)_3C_5H_2]_2UO$, and its adduct $[\eta^5\text{-}1,2,4\text{-}(Me_3C)_3C_5H_2]_2UO(OCPh_2)$.[3e] The addition of pyridine, 4-$Me_2NC_5H_4N$ (dmap), or THF to this solution yields the stable monomeric adducts, $[\eta^5\text{-}1,2,4\text{-}(Me_3C)_3C_5H_2]_2UO(py)$ and $[\eta^5\text{-}1,2,4\text{-}(Me_3C)_3C_5H_2]_2UO(dmap)$, which can be isolated, but no THF adduct $[\eta^5\text{-}1,2,4\text{-}(Me_3C)_3C_5H_2]_2UO(THF)$ is formed.[3e] In contrast, under similar reaction conditions, treatment of **4** with 1 or 2 equiv of Ph_2CO results in the isolation of the metallocenes, $\{[\eta^5\text{-}1,2,4\text{-}(Me_3C)_3C_5H_2]_2Th\}_2(\mu\text{-}O)_2$ (**6**) and $[\eta^5\text{-}1,2,4\text{-}(Me_3C)_3C_5H_2]_2Th[(\mu\text{-}O)_2(CPh_2)]$ (**7**), respectively. In both cases, the oxo metallocene $[\eta^5\text{-}1,2,4\text{-}(Me_3C)_3C_5H_2]_2ThO$ (**5**) has undergone an irreversible nucleophilic addition (Scheme 2). However, when the reaction of **4** with 1 equiv of Ph_2CO is carried out in C_6D_6 solution in the presence of THF, pyridine, or 4-$Me_2NC_5H_4N$, the corresponding adducts, $[\eta^5\text{-}1,2,4\text{-}(Me_3C)_3C_5H_2]_2ThO(s)$ (s = THF (**8**), py (**9**), dmap (**10**)), are formed (Scheme 3). The adducts **8** and **9** are stable at ambient temperature in C_6D_6 solution as monitored by ^1H NMR spectroscopy, but the dimeric μ-oxo metallocene **6** is formed when the solvent is removed or when the solution is heated. In contrast, the adduct $[\eta^5\text{-}1,2,4\text{-}(Me_3C)_3C_5H_2]_2ThO(dmap)$ (**10**) may be isolated at room temperature, but it degrades to **6** in solution at 65 °C. These observations show that the stability of actinide oxo metallocenes is very sensitive to

Scheme 3

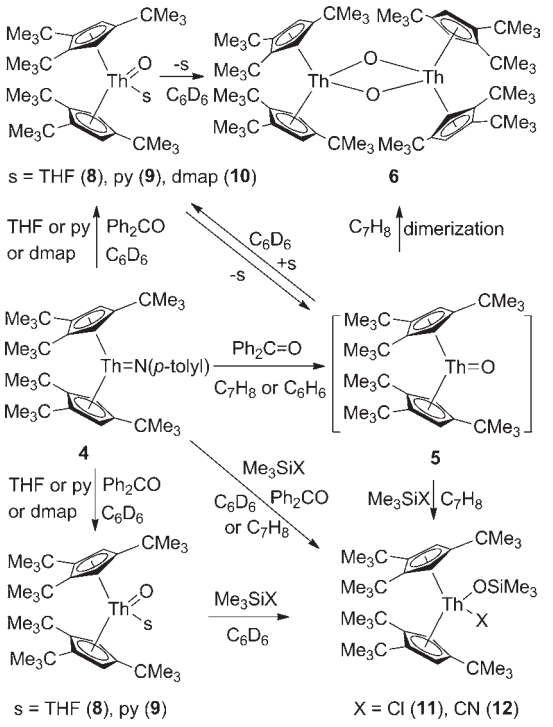

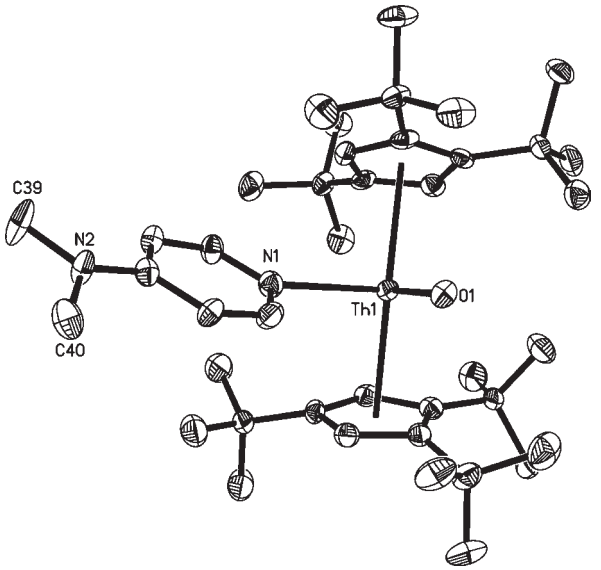

Figure 1. Molecular structure of **10** (thermal ellipsoids drawn at the 35% probability level).

the size of the metal ion[12] and the electron-donating capability of the coordinated Lewis base.[3d,e]

The uranium oxo metallocene $[\eta^5\text{-}1,2,4\text{-}(Me_3C)_3C_5H_2]_2UO$ and its adduct, $[\eta^5\text{-}1,2,4\text{-}(Me_3C)_3C_5H_2]_2UO(py)$, reacted immediately upon mixing with an excess of alkylsilyl halides to give the addition products at room temperature, but no cycloaddition behavior was observed with alkynes.[3e] The thorium oxo derivative $[\eta^5\text{-}1,2,4\text{-}(Me_3C)_3C_5H_2]_2ThO$ (**5**) and its adducts **8**−**10** behave similarly. Direct treatment of either 1 or 2 equiv of benzophenone with a mixture of **4** and Me_3SiX in toluene forms rapidly the metallocenes, $[\eta^5\text{-}1,2,4\text{-}(Me_3C)_3C_5H_2]_2Th(OSiMe_3)(X)$ (X = Cl (**11**), CN (**12**)) (Scheme 3). Treatment of C_6D_6 solutions of **8**, **9**, or **10** with an excess of Me_3SiX also cleanly yields the metallocenes **11** and **12** (Scheme 3). When heated at 65 °C, **11** can further react with an excess of Me_3SiCl to give **1**. However, the dimeric oxo metallocene **6** exhibits no reaction with an excess of Me_3SiX in C_6D_6 even when heated at 65 °C for 3 days, while **7** reacts rapidly with an excess of Me_3SiCl to form **1**. This indicates that the formation of **6** and **7** is irreversible and the active species in above reactions is the monomeric oxo metallocene **5**. However, in contrast to $(\eta^5\text{-}C_5Me_5)_2TiO(py)$,[8a] no reaction occurs when a C_6D_6 solution of **8** or **9** is treated with an excess of alkynes R′C≡CR′ (R′ = Me, Ph, Me_3Si) at room temperature, and when the temperature is increased to 65 °C dimer **6** is formed in quantitative yield, due to the more polarized nature of the actinide oxo bond.[13] When **4** is added directly to a C_6D_6 solution of benzophenone and alkynes R′C≡CR′ (R′ = Me, Ph, Me_3Si), **6** is formed in quantitative yield, indicating that the oxo **5** cannot be trapped by alkynes in contrast to $(\eta^5\text{-}C_5Me_5)_2ZrO$.[8b] This is again consistent with the more polarized An^+-O^- bond.[13] When a terminal alkyne PhC≡CH is used, proton transfer is observed accompanied by the formation of free ligand, $(Me_3C)_3C_5H_3$. In contrast to $[\eta^5\text{-}1,2,4\text{-}(Me_3C)_3C_5H_2]_2U{=}O$,[3e] the thorium derivative **5** and its adducts **8**−**10** do not react with aryl and alkyl halides. This implies that the Th=O bond is less active than the U=O bond. A similar conclusion can be derived from the fact that the heterogeneous reaction of solid U_3O_8 with chlorocarbons is fast at moderate temperature (<400 °C),[6] while the reaction of ThO_2 with CCl_4 requires high temperatures of 450−500 °C.[14]

An ORTEP diagram of $[\eta^5\text{-}1,2,4\text{-}(Me_3C)_3C_5H_2]_2ThO(dmap)$ (**10**) is shown in Figure 1. The orientation of the Cp-rings is nearly staggered, and the dmap ligand and oxygen atom lie in the open wedge of the bent metallocene. The dmap ligand is nearly planar with the dihedral angle defined by intersection of the planar pyridine ring and the plane NMe_2 group as 14°, with the planar pyridine ring twisted out of the plane defined by the Th−N−O atoms. Thus, the molecule has no symmetry in the solid state. The oxo adduct **10** represents, to the best of our knowledge, the first structurally characterized terminal oxo thorium metallocene. The Th−O distance is short with 1.929(4) Å, supporting the formation of a terminal oxo−metal bond,[15] although it is longer than that found in thorium oxide, ThO (gas phase) (1.84 Å).[16] Furthermore, it is longer than the U=O bonds found in $(\eta^5\text{-}C_5Me_5)_2U(O)(O\text{-}2,6\text{-}i\text{-}Pr_2C_6H_3)$ (1.859(6) Å),[3b] $(\eta^5\text{-}C_5Me_5)_2U(O)(N\text{-}2,6\text{-}i\text{-}Pr_2C_6H_3)$ (1.844(4) Å),[3c] $(\eta^5\text{-}C_5Me_5)_2U(O)[C(NMeCMe)_2]$ (1.917(6) Å),[3d] $[\eta^5\text{-}1,2,4\text{-}(Me_3C)_3C_5H_2]_2UO(dmap)$ (1.860(3) Å),[3e] and the Zr=O bond found in $(\eta^5\text{-}Me_4C_5Et)_2ZrO(py)$ (1.804(4) Å),[8c] but shorter than the Th=N bond found in $(\eta^5\text{-}C_5Me_5)_2Th{=}N(2,6\text{-}Me_2C_6H_3)(thf)$ (2.045(8) Å).[17] The Th−N(dmap) distance is 2.587(5) Å, which is shorter than those found in $Th(O\text{-}2,6\text{-}Me_2C_6H_3)_4(py)_2$ (2.662(8) and 2.696(8) Å),[18] $Th(OCMe_3)_4(py)_2$ (2.752(7) Å),[19] and longer than the U−N bond found in $[\eta^5\text{-}1,2,4\text{-}(Me_3C)_3C_5H_2]_2UO(dmap)$ (2.535(4) Å),[3e] and Zr−N bond found in $(\eta^5\text{-}Me_4C_5Et)_2ZrO(py)$ (2.363(5) Å).[8c]

The solid-state crystal structures of $[\eta^5\text{-}1,2,4\text{-}(Me_3C)_3C_5H_2]_2Th(OSiMe_3)(Cl)$ (**11**) and $[\eta^5\text{-}1,2,4\text{-}(Me_3C)_3C_5H_2]_2Th(OSiMe_3)(CN)$ (**12**) have been determined, and the ORTEP diagram for **12** is shown in Figure 2, whereas the ORTEP presentation for **11** is given in the Supporting Information. In each molecule, the Th^{4+}

ion coordinated in a distorted-tetrahedral geometry by two η^5-bound Cp-rings and by one σ-bound oxygen atom and by one σ-bound chlorine atom (for **11**) or one nitrogen atom (for **12**). The average Th−C(ring) distance is 2.861(3) Å for **11** and 2.849(4) Å for **12**, respectively (Table 1). The cyclopentadienyl rings in these two metallocenes adopt a nearly eclipsed conformation, with the Me_3C-groups on each ring at the back of the wedge located as far from each other as possible. This orientation sets the disposition of the other four Me_3C-groups such that two of them pointing toward the open wedge are nearly eclipsed. The Th−O−Si angle is 166.1(2)° for **11**, which is close to that (168.3(2)°) in **12**, but it is larger than the angle of U−O−Si found in $[\eta^5$-1,2,4-$(Me_3C)_3C_5H_2]_2U(OSiMe_3)(CN)$ (160.6(3)°).[3e] The Th−N−C angle is 158.2(4)°, which is smaller than the angle of U−N−C found in $[\eta^5$-1,2,4-$(Me_3C)_3C_5H_2]_2U(OSiMe_3)(CN)$ (164.5(7)°).[3e] A nonlinear Th−O−Si angle is common, while a Th−N−C angle is not. A possible reason may be traced to the steric strain on the $OSiMe_3$ and CN groups imposed by the methyl groups of the CMe_3 adjacent to them.

2.3. Thorium Sulfido Metallocenes. Thorium *p*-tolylimido metallocene **4** reacts rapidly with 1 equiv of CS_2 or PhNCS to yield the metallacycles, $[\eta^5$-1,2,4-$(Me_3C)_3C_5H_2]_2$Th[N(*p*-tolyl)-C(S)−S] (**13**) and $[\eta^5$-1,2,4-$(Me_3C)_3C_5H_2]_2$Th[N(*p*-tolyl)C-(NPh)−S] (**14**), respectively (Scheme 4). In C_6D_6 solution, complex **14** is stable at 160 °C for 3 days, whereas **13** degrades irreversibly when heated at 65 °C overnight to the dimeric thorium μ-sulfido metallocene, $\{[\eta^5$-1,2,4-$(Me_3C)_3C_5H_2]_2Th\}_2$-$(\mu$-S$)_2$ (**16**). Heating a benzene solution of **13** at 65 °C in the presence of an excess of CS_2 forms the cluster, $\{[\eta^5$-1,2,4-$(Me_3C)_3C_5H_2]_2$Th(S)[$(\mu$-S$)_2$C]$\}_6$ (**17**) (Scheme 4). Complex **4** reacts irreversibly with 2 equiv of Ph_2CS at room temperature to give the complex $[\eta^5$-1,2,4-$(Me_3C)_3C_5H_2]_2$Th[$(\mu$-S$)_2CPh_2$] (**18**) (Scheme 2). These observations suggest that the monomeric thorium sulfido metallocene $[\eta^5$-1,2,4-$(Me_3C)_3C_5H_2]_2$-ThS (**15**) is unstable and undergoes an irreversible dimerization or nucleophilic addition resembling that of the thorium oxo **5**. In contrast, the monomeric zirconium sulfido complex $(\eta^5$-^{t}BuC$_5$H$_4)_2$-ZrS shows a monomer−dimer equilibrium in solution,[8e]

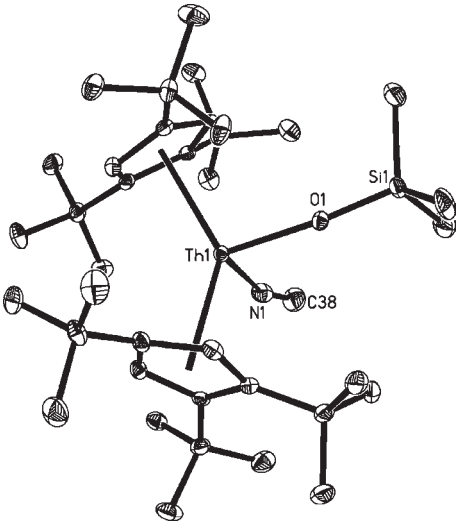

Figure 2. Molecular structure of **12** (thermal ellipsoids drawn at the 35% probability level).

Scheme 4

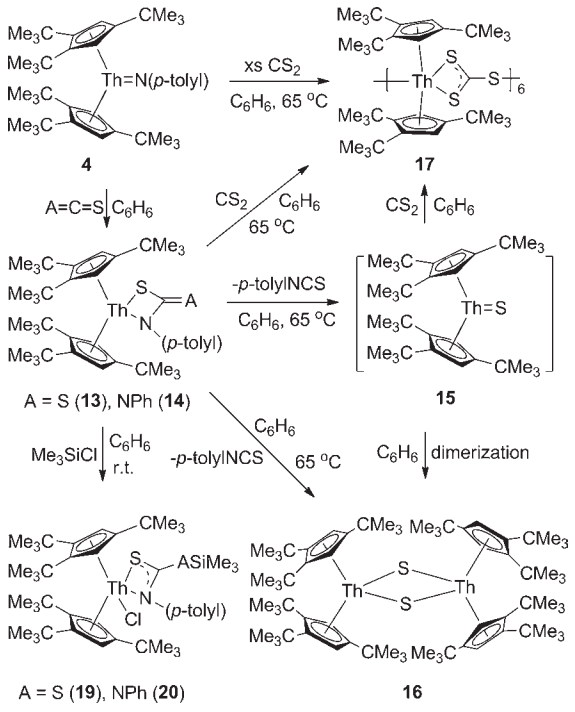

Table 1. Selected Distances (Å) and Angles (deg) for Compounds 6, 7, 10−14, 16, 17, and 19[a]

compound	C(Cp)−Th (ave)	C(Cp)−Th (range)	Cp(cent)−Th (ave)	Th−X (ave)	Cp(cent)−Th−Cp(cent)	X−Th−X (ave) or X−Th−Y
6	2.893(9)	2.776(8)−3.117(9)	2.731(9)	Th−O 2.179(6)	118.6(8), 119.3(8)	71.1(2)
7	2.898(4)	2.785(4)−3.001(4)	2.615(4)	Th−O 2.202(3), Th−C 2.741(6)	133.4(4)	62.4(2)
10	2.936(6)	2.896(6)−2.991(5)	2.676(6)	Th−O 1.929(4), Th−N 2.587(5)	142.6(6)	90.1(2)
11	2.861(3)	2.791(3)−2.916(3)	2.594(3)	Th−O 2.143(3), Th−Cl 2.647(1)	133.9(4)	91.1(1)
12	2.849(4)	2.774(4)−2.925(4)	2.580(4)	Th−O 2.132(3), Th−N 2.454(4)	136.1(4)	90.3(1)
13	2.838(7)	2.780(7)−2.935(7)	2.571(7)	Th−S 2.704(2), Th−N 2.347(6), Th−C 2.983(9)	141.0(2)	62.3(2)
14	2.853(4)	2.793(4)−2.955(4)	2.584(4)	Th−S 2.709(1), Th−N 2.328(3), Th−C 2.989(3)	140.4(3)	63.0(1)
16	2.893(9)	2.761(8)−3.098(9)	2.659(9)	Th−S 2.709(2)	119.4(1), 119.4(1)	76.8(1)
17	2.875(8)	2.777(8)−2.997(7)	2.609(8)	Th−S 2.852(2), Th−C 3.338(8)	140.2(1)	61.4(1)[b]
19	2.879(10)	2.783(9)−3.053(10)	2.615(10)	Th−S 2.890(3), Th−N 2.587(8), Th−C 3.131(9)	134.6(3)	55.9(2)[c]

[a] Cp = cyclopentadienyl ring. [b] The angle of S(1)−Th(1)−S(2). [c] The angle of S(1)−Th(1)−N(1).

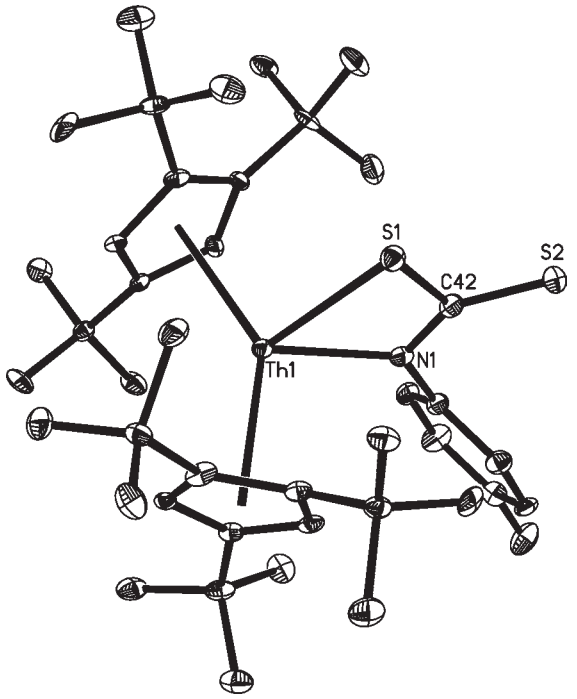

Figure 3. Molecular structure of **13** (thermal ellipsoids drawn at the 35% probability level).

suggesting that the Th^{4+} behaves more like an actinide than a transition metal.[13] Upon addition of 1 equiv of Ph_2CS to **4** in C_6D_6, the ^1H NMR spectrum of the crude reaction mixture shows resonances due to *p*-tolylN=CPh_2, new resonances attributable to $[\eta^5\text{-}1,2,4\text{-}(Me_3C)_3C_5H_2]_2Th[(\mu\text{-}S)_2CPh_2]$ (**18**), and unreacted **4**. The addition of 1 equiv of Ph_2CS to a mixture of **4** and Me_3SiCl or 4-dimethylaminopyridine (dmap) in C_6D_6 rapidly forms **18** and *p*-tolylN=CPh_2 with 50% conversion (based on **4**). Interestingly, the Lewis base dmap cannot stabilize the sulfido **15** in contrast to the oxo derivative **5**, pointing to the subtle balance between steric demand of the heteroatom anion and the electron donating capability of the Lewis base governing the reactivity and stability of the Th=X functionality. Similar to **5**, no [2 + 2] cycloaddition products $[\eta^5\text{-}1,2,4\text{-}(Me_3C)_3C_5H_2]_2$-$Th[SC(R')=C(R')]$ are obtained when **13** is heated with an excess of alkynes R′C≡CR′ (R′ = Me, Ph, Me_3Si) at 65 °C in C_6D_6 solution; instead, the μ-sulfido dimer **16** may be isolated, indicating that sulfido **15** cannot be trapped by alkynes in contrast to $(\eta^5\text{-}C_5Me_5)_2TiS(py)$[8f] and $(\eta^5\text{-}C_5Me_5)_2ZrS$,[8b] again, presumably due to the more polarized nature of the actinide sulfido bond.[13] Under similar reaction conditions, treatment of **13** or **14** with an excess of Me_3SiCl at 65 °C in a benzene solution does not give the chloride complex $[\eta^5\text{-}1,2,4\text{-}(Me_3C)_3C_5H_2]_2$-$Th(SSiMe_3)(Cl)$; instead, $[\eta^5\text{-}1,2,4\text{-}(Me_3C)_3C_5H_2]_2Th[N$-(*p*-tolyl)$C(SSiMe_3)$−S](Cl) (**19**) and $[\eta^5\text{-}1,2,4\text{-}(Me_3C)_3C_5H_2]_2$-$Th[N(p\text{-tolyl})C\{N(Ph)(SiMe_3)\}-S](Cl)$ (**20**) have been isolated (Scheme 4).

The solid-state crystal structures of **13** and **14** have been determined, and the ORTEP diagram for **13** is shown in Figure 3, whereas the ORTEP presentation for **14** is given in the Supporting Information. In each molecule, the Th^{4+} ion is η^5-bond to two Cp-rings and σ-bound to one nitrogen atom and one sulfur atom from the group [N(*p*-tolyl)C(S)−S] or [N(*p*-tolyl)C-(NPh)−S] in a distorted-tetrahedral geometry with an average

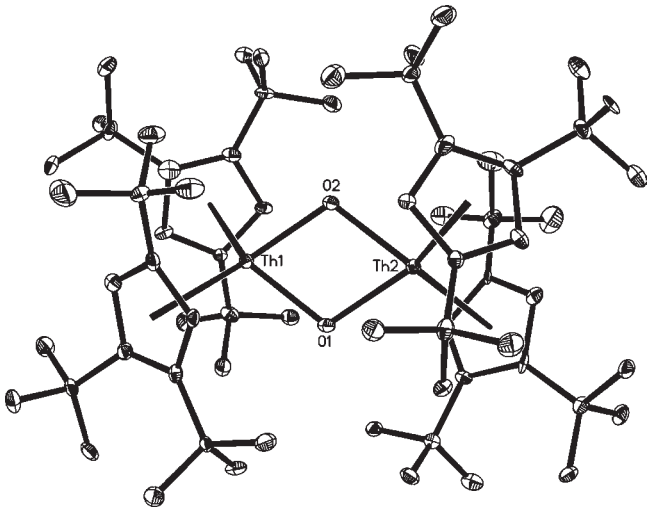

Figure 4. Molecular structure of **6** (thermal ellipsoids drawn at the 35% probability level).

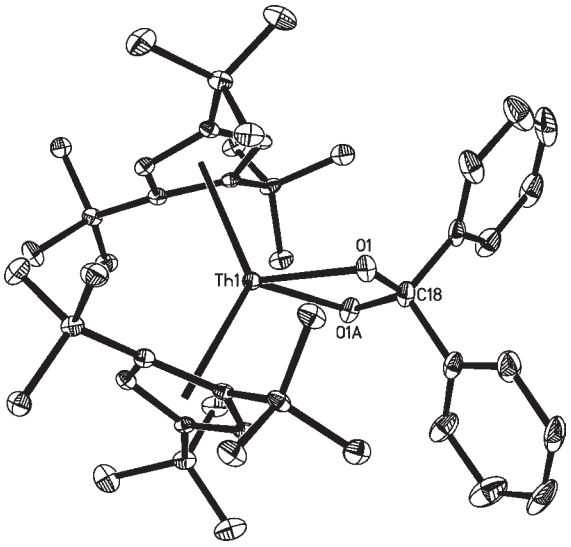

Figure 5. Molecular structure of **7** (thermal ellipsoids drawn at the 35% probability level).

Th−C(ring) distance of 2.838(7) Å for **13** and 2.853(4) Å for **14**, respectively (Table 1). The orientation of the cyclopentadienyl rings is nearly eclipsed. The structural parameters indicate that there is some charge delocalization over the N(1)−C(42)−S(1) moiety. The Cp(cent)−Th−Cp(cent) angle is 141.0(2)° for **13**, close to that (140.4(3)°) found in **14**. The Th−S distances in **13** and **14** are very similar at 2.704(2) and 2.709(1) Å, respectively. This is also reflected in the Th−N distances of 2.347(6) Å and 2.328(3) Å, respectively (Table 1).

The solid-state crystal structures of $\{[\eta^5\text{-}1,2,4\text{-}(Me_3C)_3$-$C_5H_2]_2Th\}_2(\mu\text{-}O)_2$ (**6**), $[\eta^5\text{-}1,2,4\text{-}(Me_3C)_3C_5H_2]_2Th[(\mu\text{-}O)_2$-$(CPh_2)]$ (**7**), and $\{[\eta^5\text{-}1,2,4\text{-}(Me_3C)_3C_5H_2]_2Th\}_2(\mu\text{-}S)_2$ (**16**) have been determined, and the ORTEP diagrams for **6** and **7** are shown in Figures 4 and 5, whereas the ORTEP presentation for **16** is given in the Supporting Information. The average Th−C(ring) distances are virtually identical at 2.893(9), 2.898(4), and 2.893(9) Å for **6**, **7**, and **16**, respectively

dx.doi.org/10.1021/ja205280k |*J. Am. Chem. Soc.* 2011, 133, 13183–13196

(Table 1). In each fragment of $[\eta^5\text{-}1,2,4\text{-}(Me_3C)_3C_5H_2]_2Th$, the cyclopentadienyl rings adopt a nearly staggered conformation and the Me_3C-groups at the back of the wedge are minimizing the steric repulsion, and the other four Me_3C-groups are oriented to the left and right side of the open wedge. The Cp(cent)−Th−Cp(cent) angles are 118.6(8)° and 119.3(8)° for **6**, which are close to those (119.4(1)° and 119.4(1)°) found in **16**, but smaller than that (133.4(4)°) found in **7** (Table 1). The two Th^{4+} ions are separated by 3.546(1) Å for **6**, which is longer than the U−U distance in $\{[\eta^5\text{-}1,3\text{-}(Me_3Si)_2C_5H_3]_2U\}_2(\mu\text{-}O)_2$ (3.393(1) Å),[11] consistent with the larger Th^{4+} ionic radius.[12] In **16**, the Th−Th distance is 4.246(3) Å, which can be compared to the U−U distance of 3.891(1) Å in $[Na(DME)_3]_2[\{((^{Ad}ArO)_3N)U\}_2(\mu\text{-}S)_2]$ ($(^{Ad}ArO)_3N^{3-}$ = tri-anion of tris(2-hydroxy-3-adamantyl-5-methylbenzyl)amine),[20] presumably due to the larger Th^{4+} ion in combination with the sterically more demanding $[\eta^5\text{-}1,2,4\text{-}(Me_3C)_3C_5H_2]^-$ ligand. The average Th−O distance is 2.179(6) Å for **6**, and 2.202(3) Å for **7**, which are longer than the Th=O bond (1.929(4) Å) found in **10**, but are shorter than that (2.421 Å) found in the solid-state structure of thorium dioxide, ThO_2.[21] In **16**, the average Th−S distance is 2.709(2) Å, which is shorter than that found in the organothorium complex $(\eta^5\text{-}C_5Me_5)_2ThS_5$ (2.902(4) Å),[22] and those found in the solid-state thorium sulfides, ThS (2.84 Å),[23] Th_2S_3 (2.90 Å),[24] and ThS_2 (2.95 Å).[25]

The single-crystal X-ray diffraction analysis of **17** establishes a hexanuclear cluster $\{[\eta^5\text{-}1,2,4\text{-}(Me_3C)_3C_5H_2]_2Th(S)[(\mu\text{-}S)_2C]\}_6$ (Figure 6) with six benzene solvate molecules in the crystal lattice. Each $[\eta^5\text{-}1,2,4\text{-}(Me_3C)_3C_5H_2]_2Th$ fragment is η^3-coordinated to one CS_3^{2-} fragment and σ-bound to another CS_3^{2-} fragment; thus, self-assembly of six $\{[\eta^5\text{-}1,2,4\text{-}(Me_3C)_3C_5H_2]_2Th\}^{2+}$ cations and six CS_3^{2-} anions results in the formation of a hexameric macro-ring.[26] The coordination environment in $\{[\eta^5\text{-}1,2,4\text{-}(Me_3C)_3\text{-}C_5H_2]_2Th(S)[(\mu\text{-}S)_2C]\}$ can be described as a distorted trigonal-bipyramid (Figure 6) with an average Th−C(ring) distance of 2.875(8) Å, and a Cp(cent)−Th−Cp(cent) angle of 140.2(1)°. The orientation of the cyclopentadienyl rings is nearly eclipsed as previously observed in other complexes. The small differences in the C−S distances (0.003, 0.006, and 0.009 Å) suggest that the negative charge is delocalized over the CS_3^{2-} fragment. The average Th−S distance of 2.852(2) Å is comparable to those found in **16** (2.709(2) Å), $(\eta^5\text{-}C_5Me_5)_2ThS_5$ (2.902(4) Å),[22] ThS (2.84 Å),[23] Th_2S_3 (2.90 Å),[24] and ThS_2 (2.95 Å).[25]

The single-crystal X-ray diffraction analysis of $[\eta^5\text{-}1,2,4\text{-}(Me_3C)_3C_5H_2]_2Th[N(p\text{-tolyl})C(SSiMe_3)-S](Cl)$ (**19**) reveals two independent molecules in the asymmetric unit. Each molecule possesses a distorted trigonal-bipyramidal geometry (Figure 7) with an average Th−C(ring) distance of 2.879(10) Å. The cyclopentadienyl rings adopt a nearly eclipsed conformation. The structural parameters of the $[N(p\text{-tolyl})C(SSiMe_3)-S]$ group indicate a charge delocalization over the N(1)−C(42)−S(1) unit. The Cp(cent)−Th−Cp(cent) angle is 134.6(3)°. The Th−S and Th−N distances are 2.890(3) and 2.587(8) Å, respectively. These values are similar to those listed in **13** and **14** (Table 1). The Th−Cl distance is 2.632(2) Å, identical to that found in $[\eta^5\text{-}1,3\text{-}(Me_3Si)_2C_5H_3]_2ThCl_2$,[27] but slightly shorter than that (2.647(1) Å) found in **11**.

2.4. Computational Studies. As demonstrated above, the imido complex $[\eta^5\text{-}1,2,4\text{-}(Me_3C)_3C_5H_2]_2Th{=}N(p\text{-tolyl})$ (**4**) is a useful precursor for the preparation of oxo and sulfido complexes $[\eta^5\text{-}1,2,4\text{-}(Me_3C)_3C_5H_2]_2Th{=}E$ (E = O (**5**) and S (**15**)). Complexes **5** and **15** cannot be isolated, but the reaction

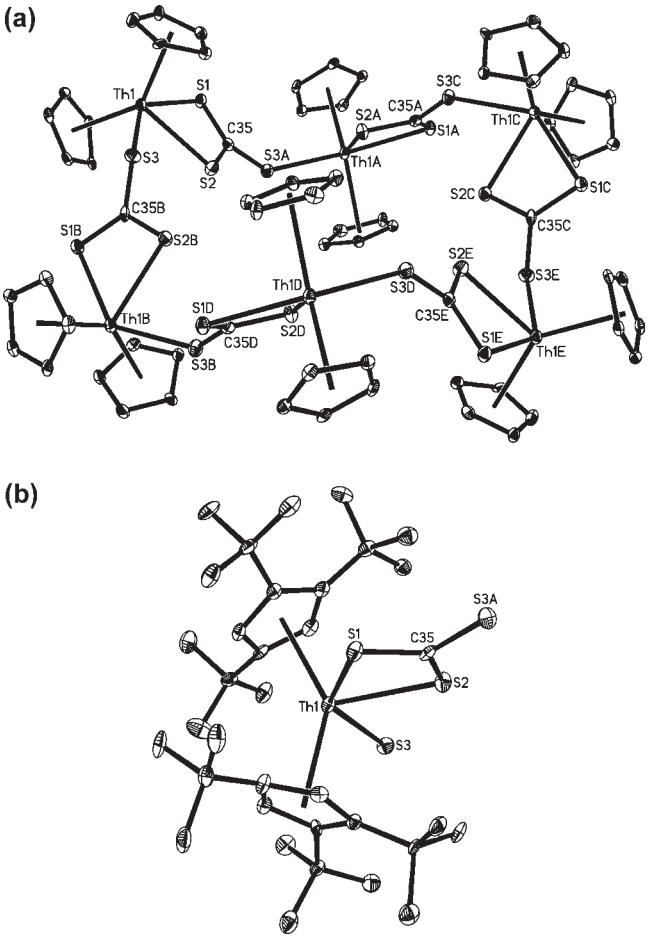

Figure 6. (a) Molecular structure of **17** (*tert*-butyl group omitted for clarity, thermal ellipsoids drawn at the 35% probability level). (b) Molecular building block of the hexameric cluster **17**.

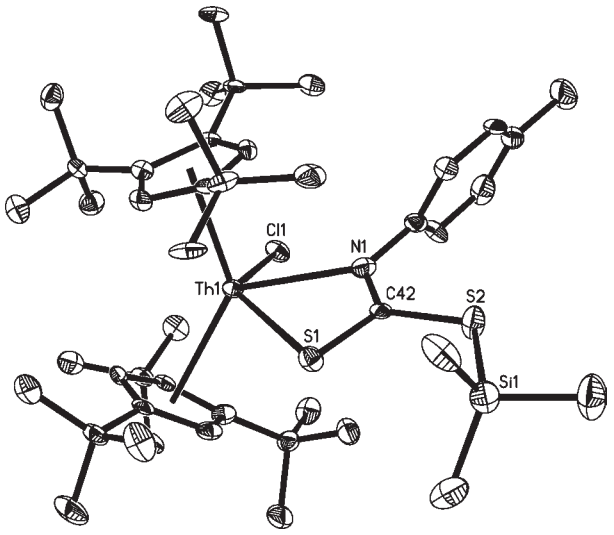

Figure 7. Molecular structure of **19** (thermal ellipsoids drawn at the 35% probability level).

chemistry has been explored. The oxo **5** acts as a nucleophile toward alkylsilyl halides, while sulfido **15** does not. The oxo **5** and sulfido **15** cannot undergo cycloaddition reactions with alkynes,

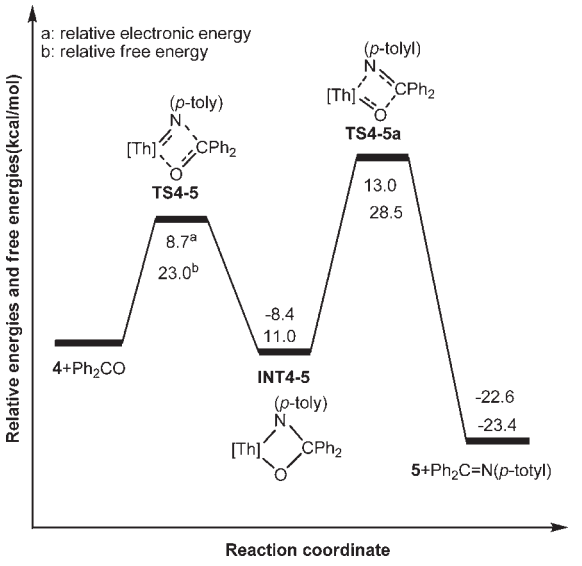

Figure 8. Energy profile (kcal mol^{-1}) for the reaction of **4** with Ph_2CO. [Th] = [η^5-1,2,4-$(Me_3C)_3C_5H_2$]$_2$Th.

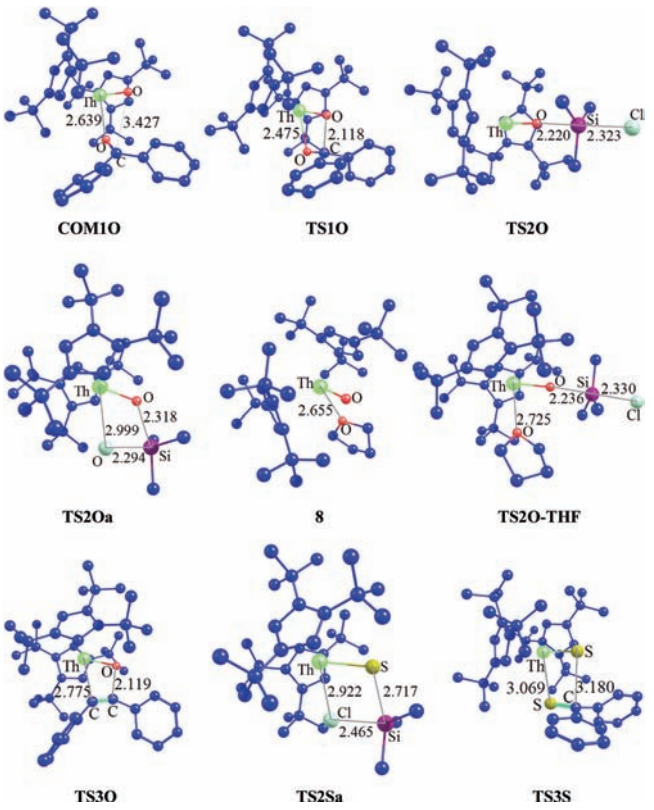

Figure 9. Optimized (B3LYP/genecp) transition state structures (TS; bond lengths in Å; the hydrogen atoms omitted for clarity) for the reaction of **5** with PhC≡CPh, Me_3SiCl, and Ph_2CO, reaction of **8** with Me_3SiCl, and reaction of **15** with Me_3SiCl and Ph_2CS.

but exhibit [2 + 2] cycloaddition behavior with Ph_2CO or Ph_2CS. To further rationalize these observations, DFT calculations have been performed.

The formation of **5** from **4**+Ph_2C═O proceeds in two steps, which involve a four-membered ring intermediate **INT4**−**5** and

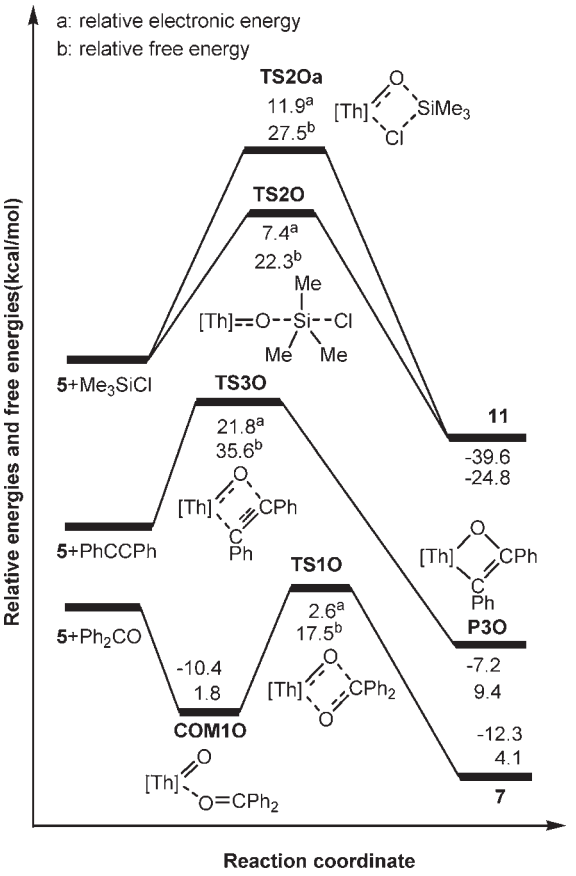

Figure 10. Energy profile (kcal mol^{-1}) for the reaction of **5** with Ph_2CO, Me_3SiCl, and PhC≡CPh. [Th] = [η^5-1,2,4-$(Me_3C)_3C_5H_2$]$_2$Th.

two transition states **TS4**−**5** and **TS4**−**5a**. Intermediate **INT4**−**5** is unstable with a Gibbs free energy of +11.0 kcal/mol relative to **4**+Ph_2C═O, but its relative electronic energy is ca. 8.4 kcal/mol lower than that of **4**+Ph_2C═O. The relative electronic energy (−22.6 kcal/mol) and free energy (−23.4 kcal/mol) of **5**+Ph_2C═N(*p*-totyl) as compared to that of **4**+Ph_2C═O indicate that the formation of **5**+Ph_2C═N(*p*-totyl) is energetically favorable (Figure 8). Furthermore, the potential energy profile suggests a short lifetime of intermediate **INT4**−**5**, consistent with the experimental observation that the **INT4**−**5** cannot be isolated from the reaction mixture. Thus, the formation of **5** is expected to proceed smoothly. However, the monomeric oxo **5** cannot be isolated due to its potential reaction with another equivalent of Ph_2CO or due to dimerization. The mechanism for the reaction of **5** with Ph_2CO involves the stable complex **COM1O** and the transition state **TS1O** (Figure 9). In **TS1O**, the two forming bond distances of Th−O and O−C are 2.475 and 2.118 Å, respectively, about 0.273 and 0.691 Å longer than those in product **7** (Table 1). Once the **COM1O** is formed, it is difficult to go back to **5**+Ph_2CO. The energy barrier for **COM1O** to **7** is 13.0 kcal/mol (Figure 10), which is readily overcome and consistent with the experimentally observed temperature of ca. 20 °C. The energy barrier of the dimerization pathway of **5** is expected to be slightly higher than that of the reaction of **5**+Ph_2C═O due to pronounced steric hindrance.

The reaction of **5** with Me_3SiCl may proceed in two different ways, that is, S_N2 (**TS2O**) and addition (**TS2Oa**) mechanisms

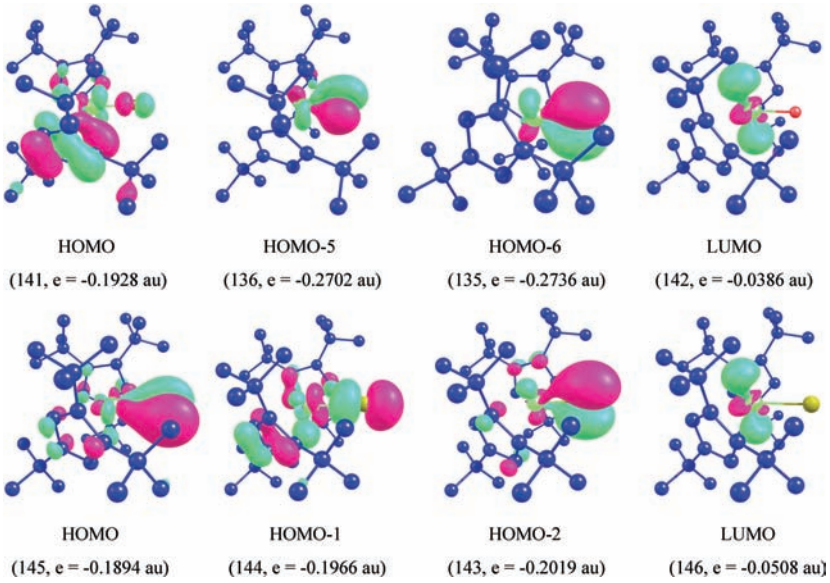

Figure 11. Isosurfaces and energies of the MOs of **5** (top) and **15** (bottom) (the hydrogen atoms omitted for clarity).

(Figure 9). The optimized bond distances of O−Si and Si−Cl in **TS2O** are 2.220 and 2.323 Å, respectively, indicating that the O−Si bond is formed and the Si−Cl bond is broken simultaneously, and the resulting Cl^- anion goes to the Th atom to form a Th−Cl bond when it leaves the Si atom. The Si atom in Me_3SiCl can readily approach the O atom, and the energy barrier for the S_N2 process is only 7.4 kcal/mol (Figure 10). Hence, the reaction can readily proceed at ambient temperature. The HOMO (Figure 11) of **5** may also account for this pathway because it is mainly the lone pair of the O atom and can therefore readily attack the Si in Me_3SiCl to release Cl^-. The addition reaction occurs via the concerted transition state **TS2Oa**, in which the two forming bond distances of Th−Cl and Si−O are 2.999 and 2.318 Å, respectively, about 0.352 and 0.673 Å longer than those in product **11** (Table 1). These combined with the Si−Cl distance of 2.294 Å indicate that the O−Si and Th−Cl bonds are formed while the Si−Cl bond is broken simultaneously. The addition reaction of **5** with Me_3SiCl has also a low activation barrier (11.9 kcal/mol) (Figure 10), but the S_N2 reaction seems to be energetically more favorable. In any case, the activation barriers for the S_N2 and the addition mechanisms are lower than that for the reaction of **5** with Ph_2CO, consistent with the experimental observations that **5** reacts faster with alkylsilyl halides than with $Ph_2C{=}O$. Furthermore, on addition of THF to a C_6D_6 solution of **5**, the adduct **8** is rapidly formed. The calculated Th−O(THF) distance is 2.655 Å, and **8** is ca. 7.8 kcal/mol more stable than **5**+THF. Reaction of **8** with Me_3SiCl can proceed in a S_N2 fashion via the transition state **TS2O-THF** (Figure 9), and the energy barrier from **8** to **11** is 12.3 kcal/mol, which is consistent with the experiment that the product **11** is readily formed on reaction of **8** with Me_3SiCl at ambient temperature. However, on coordination of a THF molecule to **5**, the *tert*-butyl groups are pushed away to accommodate the additional ligand, which increases the steric pressure between the *tert*-butyl groups on other side. Consequently, the imposed steric bulk makes the addition reaction of Me_3SiCl via **TS2Oa** less favorable.

The [2 + 2] cycloaddition of **5** with PhC≡CPh proceeds via the transition state **TS3O**, and the two forming bond distances are Th−C (2.776 Å) and C−O (2.119 Å) (Figure 9). On the basis of the frontier molecular orbital (FMO) arguments, the interaction of the HOMO−6 (Figure 11) of **5** with the LUMO of PhC≡CPh and the interaction of the LUMO (Figure 11) of **5** with the HOMO of PhC≡CPh contribute significantly to the stability of **TS3O**. The energy barrier is 21.8 kcal/mol (Figure 10), and therefore much higher than those for **5**+$Ph_2C{=}O$ and **5**+Me_3SiCl. Steric reasons make the addition reaction to an adduct of **5** such as **8** less favorable, and therefore THF dissociation must precede the cycloaddition reaction. Similar to the uranium oxo metallocene $[\eta^5\text{-}1,2,4\text{-}(Me_3C)_3C_5H_2]_2UO$,[3e] **5** can rapidly coordinate Lewis bases such as Ph_2CO to form **5**+Ph_2CO, or alternatively coordinate to another molecule of **5** to give the dimer **5**+**5**. This blocks **5** against the approach of PhC≡CPh, and the adducts **5**+Ph_2CO and **5**+**5** can then undergo cycloaddition or dimerization leading to metallacycle **7** and dimer **6**, respectively. Thus, the experimental observations are in complete agreement with the observed nucleophilicity of the polarized $Th^+{-}O^-$ moiety[13] with alkylsilyl halides, cycloaddition with Ph_2CO, or self-dimerization of the oxo **5**, but it does not undergo cycloaddition reactions with alkynes at room temperature.

The computational results may also explain the experimental observation that the sulfido **15** can easily react with $Ph_2C{=}S$ to give the cyclometallocene **18** at room temperature with the activation barrier of 8.4 kcal/mol (Figure 12). Two types of FMO interactions stabilize the transition state **TS3S** (Figure 9), the interaction of LUMO (Figure 11) of **15** with HOMO of Ph_2CS and the interaction of HOMO−2 (Figure 11) of **15** with LUMO of Ph_2CS. The transition state **TS2Sa** (Figure 9) for the addition reaction of **15** with Me_3SiCl has been located and shows an energy barrier of 18.1 kcal/mol, which is about 9.7 kcal/mol higher than that for **15**+Ph_2CS (Figure 12). Despite extensive efforts, the S_N2 transition state has not been located. This might be due to the significantly reduced nuclophilicity of **15** as compared to **5**. From the FMOs, the energy differences between lone-pair orbital (HOMO−1) and π orbitals (HOMO and HOMO −2) in **15** are −4.5 and 3.3 kcal/mol (Figure 11), respectively, while those between the lone-pair orbital (HOMO) and π orbitals (HOMO−5 and HOMO−6) in **5** are 48.6 and

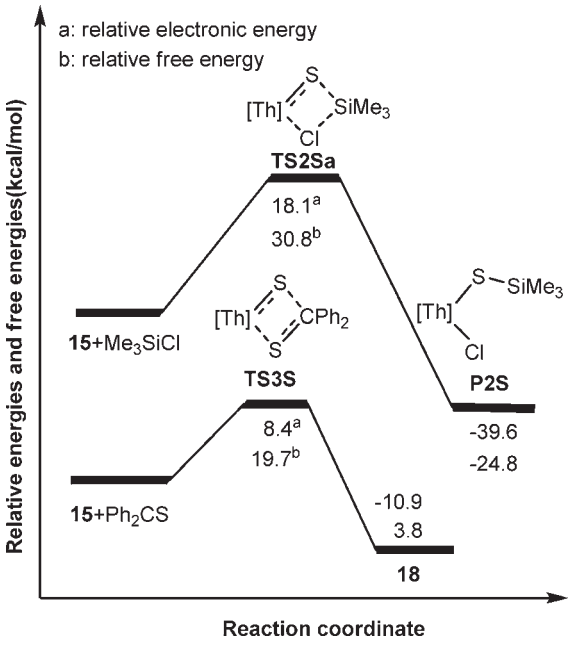

Figure 12. Energy profile (kcal/mol) for the reactions of **15**+Ph_2CS and **15**+Me_3SiCl. [Th] = $[\eta^5$-1,2,4-$(Me_3C)_3C_5H_2]_2Th$.

50.7 kcal/mol (Figure 11), respectively. Thus, the reaction of **15**+Ph_2CS becomes dominant, which is in agreement with the experimental observation that **15** does not show nucleophilic behavior toward alkylsilyl halides, but it does undergo a cycloaddition reaction with Ph_2C═S in contrast to the observations for **5**. For oxo **5**, the nucleophilic behavior with alkylsilyl halides dominates over the cycloaddition with Ph_2CO.

3. SUMMARY

Exchanging Th^{4+} for U^{4+} has a pronounced effect on the reactivity of the corresponding metallocenes. For example, the uranium(IV) oxo metallocene forms a stable pyridine adduct, $[\eta^5$-1,2,4-$(Me_3C)_3C_5H_2]_2UO(py)$,[3e] while the thorium(IV) oxo metallocene adduct, $[\eta^5$-1,2,4-$(Me_3C)_3C_5H_2]_2ThO(py)$ (**9**), is unstable. A monomer−dimer equilibrium exists for the base-free uranium oxo comples $[\eta^5$-1,2,4-$(Me_3C)_3C_5H_2]_2UO$ in solution,[3e] but the thorium derivative $[\eta^5$-1,2,4-$(Me_3C)_3C_5H_2]_2ThO$ dimerizes irreversibly to $\{\eta^5$-1,2,4-$(Me_3C)_3C_5H_2]_2Th\}_2(\mu$-$O)_2$ (**6**). Mixing $[\eta^5$-1,2,4-$(Me_3C)_3C_5H_2]_2UO$ with 1 equiv of Ph_2CO forms the adduct, $[\eta^5$-1,2,4-$(Me_3C)_3C_5H_2]_2UO(OCPh_2)$,[3e] while $[\eta^5$-1,2,4-$(Me_3C)_3C_5H_2]_2ThO$ (**5**) undergoes a [2 + 2] cycloaddition to yield $[\eta^5$-1,2,4-$(Me_3C)_3C_5H_2]_2Th[(\mu$-$O)_2(CPh_2)]$ (**7**). This shows how sensitive actinide oxo metallocenes react with respect to the size of the metal ion and the electron-donating capabilities of the Lewis base.

However, the uranium[3e] and thorium oxo metallocenes show very similar reactivity patterns; for example, both derivatives show nucleophilic behavior with alkylsilyl halides resembling that of $(\eta^5$-$C_5Me_5)_2ZrO(py)$,[8d] but they do not undergo cycloaddition reactions with alkynes in contrast to $(\eta^5$-$C_5Me_5)_2TiO(py)$[8a] and $(\eta^5$-$C_5Me_5)_2ZrO$,[8b] supporting the notion that Th^{4+} behaves more like an actinide than a transition metal.[10c] Computational studies reveal that the energy barrier of the nucleophilic substitution reaction is lower than that of cycloaddition reaction for **5**. This study may also explain the similar behavior for oxo uranium metallocenes. Furthermore, complex **5** also provides a well-defined molecular model for the heterogeneous reaction of solid ThO_2 and chlorocarbons vapor at high temperature (450−500 °C) that results in $ThCl_4$.[14]

In addition, thorium oxo and sulfido metallocenes exhibit quite different reactivity patterns; for example, $[\eta^5$-1,2,4-$(Me_3C)_3C_5H_2]_2ThO$ (**5**) can be stabilized by 4-dimethylaminopyridine (dmap), while $[\eta^5$-1,2,4-$(Me_3C)_3C_5H_2]_2ThS$ (**15**) cannot. Sulfido **15** undergoes cycloaddition with Ph_2CS, while oxo **5** exhibits increased nucleophilicity toward alkylsilyl halides and reduced cycloaddition behavior with Ph_2CO when compared to **15**. This shows that the reactivity of actinide metallocenes carrying An═E (E = heteroatom) functional groups is strongly influenced by the size of the heteroatom anion and the electronic effects associated with the An═X bonds. Furthermore, the computational studies indicate that for oxo **5**, the energy barrier for nucleophilic substitution is lower than that for the cycloaddition reaction with Ph_2CO. However, for sulfido **15**, the energy barrier of nucleophilic substitution is higher than that of the cycloaddition reaction with Ph_2CS due to the steric and electronic effects.

In conclusion, the base-free terminal imido thorium metallocene **4** is a useful precursor for the synthesis of the first terminal oxo and sulfido thorium metallocenes and enabled us to systematically probe the intrinsic reactivity of Th═E (E = O and S) bonds. These results open new ways to design and synthesize organoactinide metallocenes with terminal multiple bonds. In addition, these results should significantly expand the range of possibilities in chemical transformations not only for organoactinide oxo and sulfido complexes but also for solid-state actinide metal oxides and sulfides. We are planning to synthesize other organoactinide complexes with multiple bonds (e.g., selenido and tellurido complexes) to understand the nature of these bonds and their intrinsic reactivity. Work along these lines is currently in progress.

4. EXPERIMENTAL SECTION

General Procedures. All reactions and manipulations were carried out under an atmosphere of dry dinitrogen with rigid exclusion of air and moisture using standard Schlenk or cannula techniques, or in a glovebox. All organic solvents were freshly distilled from sodium benzophenone ketyl immediately prior to use. MeC≡CMe and CS_2 were freshly distilled from CaH_2 immediately prior to use. Me_3SiX (X = Cl, CN) were distilled under nitrogen prior to use. PhC≡CPh, Ph_2CO, and *p*-$MeC_6H_4NH_2$ were purified by sublimation. $[\eta^5$-1,2,4-$(Me_3C)_3C_5H_2]K$,[28] $ThCl_4(tmeda)_2$,[29] and Ph_2CS[30] were prepared according to literature methods. All other chemicals were purchased from Aldrich Chemical Co. and Beijing Chemical Co. used as received unless otherwise noted. Infrared spectra were obtained from KBr pellets on an Avatar 360 Fourier transform spectrometer. ^1H and $^{13}C\{^1H\}$ NMR spectra were recorded on a Bruker AV 400 spectrometer at 400 and 100 MHz, respectively. All chemical shifts were reported in δ units with reference to the residual protons of the deuterated solvents, which were internal standards, for proton and carbon chemical shifts. Melting points were measured on an X-6 melting point apparatus and were uncorrected. Elemental analyses were performed on a Vario EL elemental analyzer.

Preparation of $[\eta^5$-1,2,4-$(Me_3C)_3C_5H_2]_2ThCl_2$ (1). After a toluene (50 mL) suspension of $[\eta^5$-1,2,4-$(Me_3C)_3C_5H_2]K$ (5.00 g, 18.4 mmol) and $ThCl_4(tmeda)_2$ (5.52 g, 9.1 mmol) was refluxed for 3 days, the mixture was filtered, and the residue was washed with toluene (5 mL × 3). The volume of the filtrate was reduced to ca. 20 mL, and colorless crystals of **1** were isolated when this solution was kept at room temperature for 2 days. Yield: 5.95 g (85%). Mp: 180−182 °C. ^1H NMR

(C_6D_6): δ 6.56 (s, 4H, ring C*H*), 1.59 (s, 36H, $(CH_3)_3C$), 1.31 (s, 18H, $(CH_3)_3C$). $^{13}C\{^1H\}$ NMR (C_6D_6): δ 147.3, 146.9, 119.1, 35.3, 33.8, 33.7, 32.5. IR (KBr, cm^{-1}): ν 2955 (s), 2870 (m), 1598 (s), 1460 (s), 1391 (s), 1360 (s), 1259 (s), 1235 (s), 1018 (s), 800 (s). Anal. Calcd for $C_{34}H_{58}Cl_2Th$: C, 53.05; H, 7.59. Found: C, 53.12; H, 7.53.

Preparation of [η^5-1,2,4-$(Me_3C)_3C_5H_2]_2ThMe_2$ (2). A diethyl ether (34.6 mL) solution of MeLi (0.15 M in diethyl ether; 5.2 mmol) was slowly added to a diethyl ether (25 mL) solution of [η^5-1,2,4-$(Me_3C)_3C_5H_2]_2ThCl_2$ (**1**; 2.00 g, 2.6 mmol) with stirring at room temperature. After the solution was stirred for 1 h at room temperature, the solvent was removed. The residue was extracted with *n*-hexane (15 mL × 3) and filtered. The volume of the filtrate was reduced to ca. 10 mL and cooled to −20 °C, yielding colorless crystals, which were isolated by filtration. Yield: 1.50 g (79%). Mp: 165−170 °C (dec.). ^1H NMR (C_6D_6): δ 6.28 (s, 4H, ring C*H*), 1.54 (s, 36H, $(CH_3)_3C$), 1.26 (s, 18H, $(CH_3)_3C$), 0.46 (s, 6H, ThCH_3). $^{13}C\{^1H\}$ NMR (C_6D_6): δ 142.5, 141.2, 113.5, 58.9, 34.9, 34.2, 32.8, 32.6. IR (KBr, cm^{-1}): ν 3092 (w), 2956 (s), 2849 (s), 1611 (w), 1482 (s), 1455 (s), 1391 (s), 1358 (s), 1235 (s), 1165 (s), 1107 (s), 1000 (s), 958 (s), 824 (s), 780 (s). Anal. Calcd for $C_{36}H_{64}Th$: C, 59.32; H, 8.85. Found: C, 59.33; H, 8.78.

Preparation of [η^5-1,2,4-$(Me_3C)_3C_5H_2]_2Th(NH$-*p*-tolyl$)_2$ (3). A toluene (10 mL) solution of *p*-toluidine (0.59 g, 5.5 mmol) was added to a toluene (10 mL) solution of [η^5-1,2,4-$(Me_3C)_3C_5H_2]_2ThMe_2$ (**2**; 2.00 g, 2.75 mmol). After the mixture was stirred at 70 °C for 2 days, the solvent was removed under reduced pressure. The residue was extracted with *n*-hexane (10 mL × 3) and filtered. The volume of the filtrate was reduced to 10 mL and cooled to −20 °C, yielding colorless crystals, which were isolated by filtration. Yield: 2.25 g (90%). Mp: 136−138 °C (dec.). ^1H NMR (C_6D_6): δ 7.06 (d, J = 8.0 Hz, 4H, aryl), 6.84 (d, J = 8.0 Hz, 4H, aryl), 6.58 (s, 4H, ring C*H*), 5.07 (s, 2H, N*H*), 2.22 (s, 6H, tolylCH_3), 1.42 (s, 36H, $(CH_3)_3C$), 1.41 (s, 18H, $(CH_3)_3C$). $^{13}C\{^1H\}$ NMR (C_6D_6): δ 154.3, 144.8, 143.9, 129.5, 126.5, 119.0, 115.5, 34.9, 34.1, 33.9, 32.7, 20.5. IR (KBr, cm^{-1}): ν 3254 (m), 2962 (s), 2844 (m), 1606 (s), 1503 (s), 1448 (s), 1393 (s), 1354 (s), 1259 (s), 1162 (s), 1107 (s), 1022 (s), 957 (s), 806 (s). Anal. Calcd for $C_{48}H_{74}N_2Th$: C, 63.27; H, 8.19; N, 3.07. Found: C, 63.23; H, 8.21; N, 2.98.

Preparation of [η^5-1,2,4-$(Me_3C)_3C_5H_2]_2Th$═N(*p*-tolyl) (4). After a toluene (20 mL) solution of [η^5-1,2,4-$(Me_3C)_3C_5H_2]_2ThMe_2$ (**2**; 0.80 g, 1.1 mmol) and [η^5-1,2,4-$(Me_3C)_3C_5H_2]_2Th(NH$-*p*-tolyl$)_2$ (**3**; 1.0 g, 1.1 mmol) was refluxed for 4 days with stirring, the solution was filtered, and the volume of the filtrate was reduced to 5 mL and cooled to −20 °C, yielding colorless crystals. Yield: 1.50 g (85%). Mp: 198−200 °C. ^1H NMR (C_6D_6): δ 7.12 (d, J = 8.0 Hz, 2H, aryl), 6.52 (s, 4H, ring C*H*), 6.48 (d, J = 8.0 Hz, 2H, aryl), 2.33 (s, 3H, tolylCH_3), 1.52 (s, 36H, $(CH_3)_3C$), 1.44 (s, 18H, $(CH_3)_3C$). $^{13}C\{^1H\}$ NMR (C_6D_6): δ 158.1, 139.9, 137.7, 128.6, 123.9, 122.7, 116.8, 34.3, 33.8, 32.8, 29.8, 20.6. IR (KBr, cm^{-1}): ν 2958 (s), 1599 (s), 1471 (s), 1455 (s), 1358 (s), 1260 (s), 1235 (s), 1162 (m), 1097 (s), 1019 (s), 916 (s), 803 (s). Anal. Calcd for $C_{41}H_{65}NTh$: C, 61.25; H, 8.15; N, 1.74. Found: C, 61.23; H, 8.16; N, 1.76.

Preparation of {[η^5-1,2,4-$(Me_3C)_3C_5H_2]_2Th\}_2(\mu$-O$)_2\cdot 2C_7H_8$ ($6\cdot 2C_7H_8$). *Method A.* A toluene (5 mL) solution of benzophenone (0.12 g, 0.66 mmol) was added to a toluene (10 mL) solution of [η^5-1,2,4-$(Me_3C)_3C_5H_2]_2Th$═N(*p*-tolyl) (**4**; 0.50 g, 0.62 mmol) with stirring at room temperature. After this solution was stirred at room temperature for 0.5 h, the solution was filtered. The volume of the filtrate was reduced to 5 mL and cooled to −20 °C, yielding colorless crystals $6\cdot 2C_7H_8$, which were isolated by filtration. Yield: 0.41 g (81%). Mp: >300 °C. ^1H NMR (C_6D_6): δ 7.04 (m, 6H, tolyl), 6.95 (m, 4H, tolyl), 6.68 (s, 4H, ring C*H*), 6.08 (s, 4H, ring C*H*), 2.11 (s, 6H, tolylCH_3), 1.71 (s, 36H, $(CH_3)_3C$), 1.69 (s, 36H, $(CH_3)_3C$), 1.52 (s, 36H, $(CH_3)_3C$). $^{13}C\{^1H\}$ NMR (C_6D_6): δ 141.4, 140.8, 137.6, 136.2, 129.1, 127.5, 125.4, 115.8, 112.7, 35.9, 34.9, 34.4, 33.8, 32.8, 32.5, 21.4. IR (KBr, cm^{-1}): ν 2962 (s), 1619 (s), 1502 (s), 1446 (s), 1357 (s), 1261 (s), 1238 (s), 1093 (s), 1019 (s), 797 (s), 752 (s), 726 (s), 693 (s), 657 (s). Anal. Calcd for $C_{82}H_{132}O_2Th_2$: C, 61.02; H, 8.24. Found: C, 61.13; H, 8.22.

Method B. NMR Scale. To a J. Young NMR tube charged with a solution of [η^5-1,2,4-$(Me_3C)_3C_5H_2]_2Th$═N(*p*-tolyl) (**4**; 16 mg, 0.02 mmol) in C_6D_6 (0.5 mL) was added benzophenone (3.6 mg, 0.02 mmol). The resonances due to {[η^5-1,2,4-$(Me_3C)_3C_5H_2]_2Th\}_2(\mu$-O$)_2$ (**6**) along with those of Ph_2C═N(*p*-tolyl) ((^1H NMR (C_6D_6): δ 7.97 (m, 2H, aryl), 7.12 (m, 3H, aryl), 6.98 (m, 2H, aryl), 6.89 (m, 3H, aryl), 6.77 (m, 4H, aryl), 1.97 (s, 3H, CH_3))[3e] were observed by ^1H NMR spectroscopy (100% conversion).

Preparation of [η^5-1,2,4-$(Me_3C)_3C_5H_2]_2Th[(\mu$-O$)_2CPh_2]$ (7). *Method A.* A benzene (5 mL) solution of benzophenone (0.24 g, 1.32 mmol) was added to a benzene (10 mL) solution of [η^5-1,2,4-$(Me_3C)_3C_5H_2]_2Th$═N(*p*-tolyl) (**4**; 0.50 g, 0.62 mmol) with stirring at room temperature. After this solution was stirred overnight at room temperature, the solution was filtered. The volume of the filtrate was reduced to 5 mL and cooled to −20 °C, yielding colorless crystals **7**, which were isolated by filtration. Yield: 0.47 g (85%). Mp: 160−162 °C (dec.). ^1H NMR (C_6D_6): δ 7.84 (d, J = 7.6 Hz, 4H, aryl), 7.23 (t, J = 7.6 Hz, 4H, aryl), 7.05 (m, 2H, aryl), 6.48 (d, J = 3.2 Hz, 2H, ring C*H*), 5.93 (d, J = 3.2 Hz, 2H, ring C*H*), 1.60 (s, 18H, $(CH_3)_3C$), 1.59 (s, 18H, $(CH_3)_3C$), 1.19 (s, 18H, $(CH_3)_3C$). $^{13}C\{^1H\}$ NMR (C_6D_6): δ 151.6, 144.8, 142.5, 140.5, 129.9, 126.7, 126.5, 118.0, 116.3, 94.2, 34.9, 34.8, 33.6, 32.9, 32.4, 31.4. IR (KBr, cm^{-1}): ν 2961 (s), 1613 (s), 1592 (s), 1446 (s), 1359 (s), 1260 (s), 1069 (s), 1016 (s), 801 (s), 745 (s), 698 (s), 671 (s). Anal. Calcd for $C_{47}H_{68}O_2Th$: C, 62.93; H, 7.64. Found: C, 63.13; H, 7.62.

Method B. NMR Scale. To a J. Young NMR tube charged with a solution of [η^5-1,2,4-$(Me_3C)_3C_5H_2]_2Th$═N(*p*-tolyl) (**4**; 16 mg, 0.02 mmol) in C_6D_6 (0.5 mL) was added benzophenone (7.2 mg, 0.04 mmol). The resonances due to [η^5-1,2,4-$(Me_3C)_3C_5H_2]_2Th[(\mu$-O$)_2CPh_2]$ (**7**) along with those of Ph_2C═N(*p*-tolyl) were observed by ^1H NMR spectroscopy (100% conversion).

Reaction of [η^5-1,2,4-$(Me_3C)_3C_5H_2]_2Th[(\mu$-O$)_2CPh_2]$ (7) with Me_3SiCl. NMR Scale. To a J. Young NMR tube charged with [η^5-1,2,4-$(Me_3C)_3C_5H_2]_2Th[(\mu$-O$)_2CPh_2]$ (**7**; 18 mg, 0.02 mmol) and C_6D_6 (0.5 mL) was added an excess of Me_3SiCl. The resonances due to [η^5-1,2,4-$(Me_3C)_3C_5H_2]_2ThCl_2$ (**1**) along with those of $Ph_2C(OSiMe_3)_2$ ((^1H NMR (C_6D_6): δ 7.68 (d, J = 7.4 Hz, 2H, aryl), 7.08 (m, 8H, aryl), 0.18 (s, 18H, $(CH_3)_3Si$)) were observed by ^1H NMR spectroscopy (100% conversion).

Preparation of [η^5-1,2,4-$(Me_3C)_3C_5H_2]_2ThO$(THF) (8). NMR Scale. To a J. Young NMR tube charged with [η^5-1,2,4-$(Me_3C)_3C_5H_2]_2Th$═N(*p*-tolyl) (**4**; 16 mg, 0.02 mmol), C_6D_6 (0.5 mL), and an excess of THF was added benzophenone (3.6 mg, 0.02 mmol). The resonances due to [η^5-1,2,4-$(Me_3C)_3C_5H_2]_2Th$(O)(THF) (**8**) (^1H NMR (C_6D_6): δ 6.46 (d, J = 3.2 Hz, 2H, ring C*H*), 5.87 (d, J = 3.2 Hz, 2H, ring C*H*), 3.56 (m, THF),1.58 (s, 18H, $(CH_3)_3C$), 1.57 (s, 18H, $(CH_3)_3C$), 1.45 (m, THF), 1.14 (s, 18H, $(CH_3)_3C$)) along with those of Ph_2C═N(*p*-tolyl) were observed by ^1H NMR spectroscopy (100% conversion). No change was detected by ^1H NMR spectroscopy when the sample was kept at room temperature for 1 week. However, when the solvent was removed or this solution was heated at 65 °C, resonances due to {[η^5-1,2,4-$(Me_3C)_3C_5H_2]_2Th\}_2(\mu$-O$)_2$ (**6**) were observed by ^1H NMR spectroscopy (100% conversion).

Preparation of [η^5-1,2,4-$(Me_3C)_3C_5H_2]_2ThO$(py) (9). NMR Scale. To a J. Young NMR tube charged with [η^5-1,2,4-$(Me_3C)_3C_5H_2]_2Th$═N(*p*-tolyl) (**4**; 16 mg, 0.020 mmol), C_6D_6 (0.5 mL), and an excess of pyridine was added benzophenone (3.6 mg, 0.02 mmol). The resonances due to [η^5-1,2,4-$(Me_3C)_3C_5H_2]_2Th$(O)(py) (**9**) (^1H NMR (C_6D_6): δ 8.78 (m, py), 6.94 (m, py), 6.64 (m, py), 6.48 (d, J = 3.4 Hz, 2H, ring C*H*), 5.92 (d, J = 3.4 Hz, 2H, ring C*H*), 1.60 (s, 18H, $(CH_3)_3C$), 1.59 (s, 18H, $(CH_3)_3C$), 1.18 (s, 18H, $(CH_3)_3C$)) along

with those of $Ph_2C{=}N(p\text{-tolyl})$ were observed by ^1H NMR spectroscopy (100% conversion). No change was detected by ^1H NMR spectroscopy when the sample was kept at room temperature for 1 week. However, when the solvent was removed or this solution was heated at 65 °C, resonances due to $\{[\eta^5\text{-}1,2,4\text{-}(Me_3C)_3C_5H_2]_2Th\}_2(\mu\text{-}O)_2$ (**6**) were observed by ^1H NMR spectroscopy (100% conversion).

Preparation of $[\eta^5\text{-}1,2,4\text{-}(Me_3C)_3C_5H_2]_2ThO(dmap)$ (10). A THF (5 mL) solution of benzophenone (120 mg, 0.66 mmol) was added to a THF (10 mL) solution of $[\eta^5\text{-}1,2,4\text{-}(Me_3C)_3C_5H_2]_2Th{=}N(p\text{-tolyl})$ (**4**; 500 mg, 0.62 mmol) and 4-dimethylaminopyridine (dmap; 80 mg, 0.65 mmol) with stirring at room temperature. After this solution was stirred at room temperature for 0.5 h, the solution was filtered. The volume of the filtrate was reduced to 5 mL and cooled to −20 °C, yielding colorless crystals **10**, which were isolated by filtration. Yield: 415 mg (75%). Mp: 138−140 °C (dec.). ^1H NMR (C_6D_6): δ 8.88 (s, 2H, dmap), 6.40 (s, 2H, ring C*H*), 6.34 (s, 2H, ring C*H*), 5.99 (s, 2H, dmap), 1.99 (s, 6H, NCH_3), 1.89 (s, 18H, $(CH_3)_3C$), 1.78 (s, 18H, $(CH_3)_3C$), 1.29 (s, 18H, $(CH_3)_3C$). $^{13}C\{^1H\}$ NMR (C_6D_6): δ 152.5, 139.1, 138.9, 138.2, 129.1, 113.4, 113.0, 106.3, 44.6, 37.9, 35.5, 35.0, 33.9, 32.7, 32.6. IR (KBr, cm^{-1}): ν 2961 (m), 1612 (s), 1445 (m), 1391 (m), 1352 (m), 1260 (s), 1089 (s), 1019 (s), 1002 (s), 801 (s), 724 (s). Anal. Calcd for $C_{41}H_{68}N_2OTh$: C, 58.83; H, 8.19; N, 3.35. Found: C, 58.78; H, 8.21; N, 3.36. No change was detected by ^1H NMR spectroscopy when a sample of **10** was kept at room temperature for 1 week. However, when the sample was heated at 65 °C, resonances due to $\{[\eta^5\text{-}1,2,4\text{-}(Me_3C)_3C_5H_2]_2Th\}_2(\mu\text{-}O)_2$ (**6**) were observed by ^1H NMR spectroscopy (100% conversion).

Preparation of $[\eta^5\text{-}1,2,4\text{-}(Me_3C)_3C_5H_2]_2Th(OSiMe_3)(Cl)$ (11). *Method A.* A toluene (5 mL) solution of benzophenone (0.12 g, 0.66 mmol) was added to a toluene (20 mL) solution of $[\eta^5\text{-}1,2,4\text{-}(Me_3C)_3C_5H_2]_2Th{=}N(p\text{-tolyl})$ (**4**; 0.50 g, 0.62 mmol) and Me_3SiCl (1.0 mL) with stirring at room temperature. After the solution was stirred at room temperature for 1 h, the solvent was removed. The residue was extracted with *n*-hexane (10 mL × 3) and filtered. The volume of the filtrate was reduced to 5 mL and cooled to −20 °C, yielding colorless crystals, which were isolated by filtration. Yield: 0.43 g (84%). Mp: 220−222 °C (dec.). ^1H NMR (C_6D_6): δ 6.40 (d, J = 3.2 Hz, 2H, ring C*H*), 6.38 (d, J = 3.2 Hz, 2H, ring C*H*), 1.62 (s, 18H, $(CH_3)_3C$), 1.56 (s, 18H, $(CH_3)_3C$), 1.40 (s, 18H, $(CH_3)_3C$), 0.35 (s, 9H, $(CH_3)_3Si$). $^{13}C\{^1H\}$ NMR (C_6D_6): δ 145.4, 144.5, 144.3, 118.9, 115.6, 35.1, 34.5, 34.1, 34.0, 33.9, 32.3, 3.2. IR (KBr, cm^{-1}): ν 2959 (m), 2904 (m), 2868 (m), 1482 (s), 1455 (s), 1390 (s), 1358 (s), 1260 (s), 1236 (s), 1163 (s), 1095 (s), 1021 (s), 892 (s), 805 (s). Anal. Calcd for $C_{37}H_{67}ClOSiTh$: C, 53.96; H, 8.20. Found: C, 54.12; H, 8.21.

Method B. NMR Scale. Benzophenone (7.2 mg, 0.04 mmol) was added to a J. Young NMR tube charged with $[\eta^5\text{-}1,2,4\text{-}(Me_3C)_3C_5H_2]_2Th{=}N(p\text{-tolyl})$ (**4**; 16 mg, 0.02 mmol), C_6D_6 (0.5 mL), and an excess of Me_3SiCl. The resonances due to $[\eta^5\text{-}1,2,4\text{-}(Me_3C)_3C_5H_2]_2Th(OSiMe_3)(Cl)$ (**11**) along with those of $Ph_2C{=}N(p\text{-tolyl})$ were observed by ^1H NMR spectroscopy (100% conversion). This sample was maintained at 65 °C and monitored periodically by ^1H NMR spectroscopy. After 1 day, conversion to $[\eta^5\text{-}1,2,4\text{-}(Me_3C)_3C_5H_2]_2ThCl_2$ (**1**) was 65%, and after 2 days, complete conversion to $[\eta^5\text{-}1,2,4\text{-}(Me_3C)_3C_5H_2]_2ThCl_2$ (**1**) was achieved.

Method C. NMR Scale. Benzophenone (3.6 mg, 0.02 mmol) was added to a J. Young NMR tube charged with $[\eta^5\text{-}1,2,4\text{-}(Me_3C)_3C_5H_2]_2Th{=}N(p\text{-tolyl})$ (**4**; 16 mg, 0.02 mmol), C_6D_6 (0.5 mL), and an excess of pyridine. After 10 min, an excess of Me_3SiCl was added to the mixture. The resonances due to $[\eta^5\text{-}1,2,4\text{-}(Me_3C)_3C_5H_2]_2Th(OSiMe_3)(Cl)$ (**11**) along with those of $Ph_2C{=}N(p\text{-tolyl})$ were observed by ^1H NMR spectroscopy (100% conversion).

Preparation of $[\eta^5\text{-}1,2,4\text{-}(Me_3C)_3C_5H_2]_2Th(OSiMe_3)(CN)$ (12). *Method A.* This compound was prepared as colorless crystals from the reaction of $[\eta^5\text{-}1,2,4\text{-}(Me_3C)_3C_5H_2]_2Th{=}N(p\text{-tolyl})$ (**4**; 0.5 g, 0.62 mmol) and Me_3SiCN (1.0 mL) and benzophenone (0.12 g, 0.66 mmol) in toluene (25 mL) and recrystallization from an *n*-hexane solution by a procedure similar to that in the synthesis of **11** (method A). Yield: 0.40 g (80%). Mp: 203−205 °C (dec.). ^1H NMR (C_6D_6): δ 6.33 (s, 2H, ring C*H*), 6.30 (s, 2H, ring C*H*), 1.61 (s, 18H, $(CH_3)_3C$), 1.51 (s, 18H, $(CH_3)_3C$), 1.38 (s, 18H, $(CH_3)_3C$), 0.34 (s, 9H, $(CH_3)_3Si$). $^{13}C\{^1H\}$ NMR (C_6D_6): δ 145.8, 145.2, 144.7, 130.0, 118.8, 116.1, 34.9, 34.3, 34.2, 34.0, 33.7, 32.2, 3.3. IR (KBr, cm^{-1}): ν 2961 (m), 2850 (m), 2039 (m), 1449 (m), 1260 (s), 1090 (s), 1019 (s), 798 (s). Anal. Calcd for $C_{38}H_{67}NOSiTh$: C, 56.06; H, 8.30; N, 1.72. Found: C, 56.00; H, 8.28; N, 1.67.

Method B. NMR Scale. Benzophenone (3.6 mg, 0.02 mmol) was added to a J. Young NMR tube charged with $[\eta^5\text{-}1,2,4\text{-}(Me_3C)_3C_5H_2]_2Th{=}N(p\text{-tolyl})$ (**4**; 16 mg, 0.02 mmol), C_6D_6 (0.5 mL), and an excess of THF. After 10 min, an excess of Me_3SiCN was added to the mixture. The resonances due to $[\eta^5\text{-}1,2,4\text{-}(Me_3C)_3C_5H_2]_2Th(OSiMe_3)(CN)$ (**12**) along with those of $Ph_2C{=}N(p\text{-tolyl})$ were observed by ^1H NMR spectroscopy (100% conversion).

Reaction of $\{[\eta^5\text{-}1,2,4\text{-}(Me_3C)_3C_5H_2]_2Th\}_2(\mu\text{-}O)_2$ (6) with Me_3SiX (X = Cl, CN). NMR Scale. To a J. Young NMR tube charged with $\{[\eta^5\text{-}1,2,4\text{-}(Me_3C)_3C_5H_2]_2Th\}_2(\mu\text{-}O)_2$ (**6**; 16 mg, 0.01 mmol) and C_6D_6 (0.5 mL) was added an excess of Me_3SiX (X = Cl, CN). In each case, the sample was monitored periodically by ^1H NMR spectroscopy, and no change was detected in the ^1H NMR spectrum when the sample was heated at 65 °C for 3 days.

Reaction of $[\eta^5\text{-}1,2,4\text{-}(Me_3C)_3C_5H_2]_2ThO(THF)$ (8) or $[\eta^5\text{-}1,2,4\text{-}(Me_3C)_3C_5H_2]_2ThO(py)$ (9) with $R'C{\equiv}CR'$ (R′ = Me, Ph, Me_3Si), $CH_2{=}CH_2$, Me_3CCl, or C_6H_5Cl. NMR Scale. Benzophenone (3.6 mg, 0.02 mmol) was added to a J. Young NMR tube charged with $[\eta^5\text{-}1,2,4\text{-}(Me_3C)_3C_5H_2]_2Th{=}N(p\text{-tolyl})$ (**4**; 16 mg, 0.02 mmol), C_6D_6 (0.5 mL), and an excess of THF or pyridine. After 10 min, an excess of $R'C{\equiv}CR'$ (R′ = Me, Ph, Me_3Si), $CH_2{=}CH_2$, Me_3CCl, or C_6H_5Cl was added. In each case, the sample was monitored periodically by ^1H NMR spectroscopy, and the spectrum did not show any change when kept at room temperature for 3 days. However, when the solution was heated at 65 °C, resonances due to $\{[\eta^5\text{-}1,2,4\text{-}(Me_3C)_3C_5H_2]_2Th\}_2(\mu\text{-}O)_2$ (**6**) were observed by ^1H NMR spectroscopy (100% conversion).

Reaction of $[\eta^5\text{-}1,2,4\text{-}(Me_3C)_3C_5H_2]_2ThO$ (5) with $R'C{\equiv}CR'$ (R′ = Me, Ph, Me_3Si). NMR Scale. $[\eta^5\text{-}1,2,4\text{-}(Me_3C)_3C_5H_2]_2Th{=}N(p\text{-tolyl})$ (**4**; 16 mg, 0.02 mmol) was added to a J. Young NMR tube charged with benzophenone (3.6 mg, 0.02 mmol), C_6D_6 (0.5 mL), and an excess of $R'C{\equiv}CR'$ (R′ = Me, Ph, Me_3Si). In each case, the resonances due to $\{[\eta^5\text{-}1,2,4\text{-}(Me_3C)_3C_5H_2]_2Th\}_2(\mu\text{-}O)_2$ (**6**) along with those of $Ph_2C{=}N(p\text{-tolyl})$ were observed by ^1H NMR spectroscopy (100% conversion). Each sample was monitored periodically by ^1H NMR spectroscopy, and no change was detected by ^1H NMR spectroscopy when the sample was heated at 65 °C for 3 days.

Reaction of $[\eta^5\text{-}1,2,4\text{-}(Me_3C)_3C_5H_2]_2ThO$ (5) with Me_3CCl or C_6H_5Cl. NMR Scale. Benzophenone (3.6 mg, 0.02 mmol) was added to a J. Young NMR tube charged with $[\eta^5\text{-}1,2,4\text{-}(Me_3C)_3C_5H_2]_2Th{=}N(p\text{-tolyl})$ (**4**; 16 mg, 0.02 mmol), C_6D_6 (0.5 mL), and an excess of Me_3CCl or C_6H_5Cl. In each case, the resonances due to $\{[\eta^5\text{-}1,2,4\text{-}(Me_3C)_3C_5H_2]_2Th\}_2(\mu\text{-}O)_2$ (**6**) along with those of $Ph_2C{=}N(p\text{-tolyl})$ were observed by ^1H NMR spectroscopy (100% conversion). Each sample was monitored periodically by ^1H NMR spectroscopy, and no change was detected by ^1H NMR spectroscopy when the sample was heated at 65 °C for 3 days.

Reaction of $[\eta^5\text{-}1,2,4\text{-}(Me_3C)_3C_5H_2]_2ThO(THF)$ (8) or $[\eta^5\text{-}1,2,4\text{-}(Me_3C)_3C_5H_2]_2ThO(py)$ (9) with $PhC{\equiv}CH$. NMR Scale. Benzophenone (3.6 mg, 0.02 mmol) was added to a J. Young NMR tube charged with $[\eta^5\text{-}1,2,4\text{-}(Me_3C)_3C_5H_2]_2Th{=}N(p\text{-tolyl})$ (**4**; 16 mg, 0.02 mmol), C_6D_6 (0.5 mL), and an excess of THF or pyridine. After 10

min, an excess of PhC≡CH was added. In each case, the resonances due to $(Me_3C)_3C_5H_3$[3e] and resonances due to other unidentified thorium containing compounds were observed by ^{1}H NMR spectroscopy (100% conversion).

Preparation of [η^5-1,2,4-$(Me_3C)_3C_5H_2]_2$Th[N(*p*-tolyl)C(S)−S] (13). A benzene (5 mL) solution of CS_2 (47 mg, 0.62 mmol) was added to a benzene (10 mL) solution of [η^5-1,2,4-$(Me_3C)_3C_5H_2]_2$Th═N(*p*-tolyl) (**4**; 500 mg, 0.62 mmol) with stirring at room temperature. After the mixture was stirred at room temperature for 1 h, the solution was filtered. The volume of the filtrate was reduced to 2 mL, and colorless crystals **13**·0.5C_6H_6 were isolated from the mixture after this solution stood at room temperature for 1 week. Yield: 400 mg (70%). Mp: 130−132 °C (dec.). ^{1}H NMR (C_6D_6): δ 7.50 (d, J = 8.0 Hz, 2H, aryl), 7.15 (s, 3H, C_6H_6), 7.13 (d, J = 8.0 Hz, 2H, aryl), 6.41 (d, J = 3.2 Hz, 2H, ring C*H*), 6.32 (d, J = 3.2 Hz, 2H, ring C*H*), 2.19 (s, 3H, tolylCH_3), 1.57 (s, 18H, $(CH_3)_3$C), 1.43 (s, 18H, $(CH_3)_3$C), 1.13 (s, 18H, $(CH_3)_3$C). ^{13}C{^{1}H} NMR (C_6D_6): δ 198.4, 149.0, 146.0, 145.4, 145.1, 134.1, 129.3, 128.0, 126.2, 121.5, 116.8, 36.0, 34.9, 34.7, 34.1, 33.8, 33.6, 20.7. IR (KBr, cm^{-1}): ν 2961 (s), 1502 (m), 1450 (m), 1358 (m), 1260 (s), 1090(s), 1017 (s), 971 (s), 798 (s). Anal. Calcd for $C_{45}H_{68}NS_2Th$: C, 58.80; H, 7.46; N, 1.52. Found: C, 58.65; H, 7.35; N, 1.56.

Preparation of [η^5-1,2,4-$(Me_3C)_3C_5H_2]_2$Th[N(*p*-tolyl)C(NPh)−S] (14). A benzene (5 mL) solution of PhNCS (84 mg, 0.62 mmol) was added to a benzene (10 mL) solution of [η^5-1,2,4-$(Me_3C)_3C_5H_2]_2$Th═N(*p*-tolyl) (**4**; 500 mg, 0.62 mmol) with stirring at room temperature. After the mixture was stirred at room temperature for 1 h, the solution was filtered. The volume of the filtrate was reduced to 2 mL, and colorless crystals **14** were isolated from the mixture after this solution stood at room temperature for 2 days. Yield: 454 mg (78%). Mp: 155−157 °C. ^{1}H NMR (C_6D_6): δ 7.63 (d, J = 8.0 Hz, 2H, aryl), 7.40 (t, J = 8.0 Hz, 2H, aryl), 7.33 (d, J = 7.2 Hz, 2H, aryl), 7.14 (d, J = 8.0 Hz, 2H, aryl), 6.99 (m, 1H, aryl), 6.47 (d, J = 3.2 Hz, 2H, ring C*H*), 6.38 (d, J = 3.2 Hz, 2H, ring C*H*), 2.20 (s, 3H, tolylCH_3), 1.55 (s, 18H, $(CH_3)_3$C), 1.42 (s, 18H, $(CH_3)_3$C), 1.22 (s, 18H, $(CH_3)_3$C). ^{13}C{^{1}H} NMR (C_6D_6): δ 152.0, 148.0, 145.8, 145.2, 145.0, 132.0, 129.2, 128.5, 128.3, 124.8, 123.6, 121.8, 120.2, 117.3, 35.6, 34.7, 33.8, 33.7, 33.6, 31.8, 20.7. IR (KBr, cm^{-1}): ν 2961 (s), 1604 (m), 1557 (s), 1453 (m), 1355 (s), 1260 (s), 1090 (s), 1023 (s), 946 (s), 798 (s). Anal. Calcd for $C_{48}H_{70}N_2STh$: C, 61.38; H, 7.51; N, 2.98. Found: C, 61.45; H, 7.45; N, 3.01. The ^{1}H NMR spectrum of the sample did not show any change when kept at 160 °C for 3 days.

Preparation of {[η^5-1,2,4-$(Me_3C)_3C_5H_2]_2$Th}$_2$(μ-S)$_2$ (16) *Method A.* After a benzene (10 mL) solution of [η^5-1,2,4-$(Me_3C)_3C_5H_2]_2$Th[N(*p*-tolyl)C(S)-S] (**13**; 190 mg, 0.2 mmol) was stirred at 65 °C overnight, the solution was filtered. The volume of the filtrate was reduced to 2 mL, and colorless crystals **16** were isolated from the mixture after this solution stood at room temperature for 2 days. Yield: 120 mg (82%). Mp: >300 °C. ^{1}H NMR (C_6D_6): δ 6.85 (d, J = 2.4 Hz, 2H, ring C*H*), 6.81 (d, J = 2.4 Hz, 2H, ring C*H*), 1.91 (s, 18H, $(CH_3)_3$C), 1.61 (s, 18H, $(CH_3)_3$C), 1.57 (s, 18H, $(CH_3)_3$C). ^{13}C{^{1}H} NMR (C_6D_6): δ 150.0, 141.5, 137.7, 126.5, 118.0, 116.3, 36.4, 35.4, 34.9, 34.2, 33.3, 33.0. IR (KBr, cm^{-1}): ν 2960 (s), 1511 (m), 1459 (m), 1363 (s), 1259 (s), 1093 (s), 1017 (s), 798 (s). Anal. Calcd for $C_{68}H_{116}S_2Th_2$: C, 55.87; H, 8.00. Found: C, 55.90; H, 7.92.

Method B. NMR Scale. An NMR sample of [η^5-1,2,4-$(Me_3C)_3C_5H_2]_2$Th[N(*p*-tolyl)C(S)-S] (**13**; 19 mg, 0.02 mmol) with C_6H_6 (0.5 mL) was monitored periodically by ^{1}H NMR spectroscopy. When the sample was heated at 65 °C for 8 h, resonances due to {[η^5-1,2,4-$(Me_3C)_3C_5H_2]_2$Th}$_2$(μ-S)$_2$ (**16**) along with those of *p*-tolylNCS ((^{1}H NMR (C_6D_6): δ 6.53 (m, 4H, aryl), 1.83 (s, 3H, tolylCH_3))[31] were observed by ^{1}H NMR spectroscopy (100% conversion).

Reaction of [η^5-1,2,4-$(Me_3C)_3C_5H_2]_2$Th[N(*p*-tolyl)C(S)-S] (13) with RC≡CR (R = Me, Ph). NMR Scale. To a J. Young NMR tube charged with [η^5-1,2,4-$(Me_3C)_3C_5H_2]_2$Th[N(*p*-tolyl)C(S)-S] (**13**; 18 mg, 0.02 mmol) and C_6D_6 (0.5 mL) was added an excess of RC≡CR (R = Me, Ph). In each case, the sample was monitored periodically by ^{1}H NMR spectroscopy. When the solution was heated at 65 °C for 8 h, resonances due to {[η^5-1,2,4-$(Me_3C)_3C_5H_2]_2$Th}$_2$-(μ-S)$_2$ (**16**) along with those of *p*-tolylNCS were observed by ^{1}H NMR spectroscopy (100% conversion).

Preparation of {[1,2,4-$(Me_3C)_3C_5H_2]_2$Th[(μ-S)$_2$CS]}$_6$·6C_6H_6 (17·6C_6H_6). CS_2 (0.5 mL) was added to a benzene (10 mL) solution of [η^5-1,2,4-$(Me_3C)_3C_5H_2]_2$Th[N(*p*-tolyl)C(S)−S] (**13**; 190 mg, 0.2 mmol). After this mixture was heated at 65 °C overnight without stirring, yellow crystals were isolated from the solution, which were identified as **17**·6C_6H_6 by X-ray diffraction analysis. Yield: 166 mg (94%). Mp: >300 °C. IR (KBr, cm^{-1}): ν 2961 (s), 1451 (m), 1357 (m), 1261 (s), 1090 (s), 1019 (s), 936 (s), 892 (s), 798 (s). Anal. Calcd for $C_{246}H_{384}S_{18}Th_6$: C, 55.63; H, 7.29. Found: C, 55.58; H, 7.31. This compound was insoluble in deuterated solvents such as pyridine, THF, toluene, and CD_2Cl_2, which made the characterization by NMR spectroscopy infeasible. This compound was also prepared in 96% yield (85 mg) from the reaction of [η^5-1,2,4-$(Me_3C)_3C_5H_2]_2$Th═N(*p*-tolyl) (**4**; 80 mg, 0.1 mmol) with an excess of CS_2 (0.2 mL) in benzene at 65 °C.

Preparation of [η^5-1,2,4-$(Me_3C)_3C_5H_2]_2$Th[(μ-S)$_2$CPh$_2$] (18). *Method A.* A benzene (5 mL) solution of Ph_2CS (0.25 g, 1.26 mmol) was added to a benzene (10 mL) solution of [η^5-1,2,4-$(Me_3C)_3C_5H_2]_2$Th═N-(*p*-tolyl) (**4**; 0.50 g, 0.62 mmol) with stirring at room temperature. After this solution was stirred for 2 h at room temperature, the solution was filtered. The volume of the filtrate was reduced to 1 mL, and pale yellow microcrystals **18** were isolated from the mixture after this solution stood at room temperature for 3 days. Yield: 0.43 g (75%). Mp: 185−187 °C (dec.). ^{1}H NMR (C_6D_6): δ 8.24 (d, J = 7.2 Hz, 4H, aryl), 7.19 (t, J = 7.2 Hz, 4H, aryl), 7.01 (t, J = 7.2 Hz, 2H, aryl), 6.48 (s, 2H, ring C*H*), 6.45 (s, 2H, ring C*H*), 1.50 (s, 36H, $(CH_3)_3$C), 1.27 (s, 18H, $(CH_3)_3$C). ^{13}C{^{1}H} NMR (C_6D_6): δ 153.3, 146.5, 145.8, 143.8, 128.9, 127.3, 125.7, 120.9, 116.6, 60.9, 35.5, 35.0, 34.0, 33.2, 32.7, 31.3. IR (KBr, cm^{-1}): ν 2962 (s), 1592 (m), 1439 (m), 1409 (m), 1260 (s), 1090 (s), 1018 (s), 798 (s). Anal. Calcd for $C_{47}H_{68}S_2Th$: C, 60.75; H, 7.38. Found: C, 60.82; H, 7.32.

Method B. NMR Scale. To a J. Young NMR tube charged with a solution of [η^5-1,2,4-$(Me_3C)_3C_5H_2]_2$Th═N(*p*-tolyl) (**4**; 16 mg, 0.02 mmol) in C_6D_6 (0.5 mL) was added Ph_2CS (4.0 mg, 0.02 mmol). The resonances due to [η^5-1,2,4-$(Me_3C)_3C_5H_2]_2$Th[(μ-S)$_2$CPh$_2$] (**18**) along with those of Ph_2C═N(*p*-tolyl) and unreacted **4** were observed by ^{1}H NMR spectroscopy (50% conversion based on **4**).

Method C. NMR Scale. Ph_2CS (4.0 mg, 0.02 mmol) was added to a J. Young NMR tube charged with [η^5-1,2,4-$(Me_3C)_3C_5H_2]_2$Th═N(*p*-tolyl) (**4**; 16 mg, 0.02 mmol), C_6D_6 (0.5 mL), and an excess of Me_3SiCl. The resonances due to [η^5-1,2,4-$(Me_3C)_3C_5H_2]_2$Th[(μ-S)$_2$CPh$_2$] (**18**) along with those of Ph_2C═N(*p*-tolyl) and unreacted **4** were observed by ^{1}H NMR spectroscopy (50% conversion based on **4**).

Method D. NMR Scale. Ph_2CS (4.0 mg, 0.02 mmol) was added to a J. Young NMR tube charged with [η^5-1,2,4-$(Me_3C)_3C_5H_2]_2$Th═N(*p*-tolyl) (**4**; 16 mg, 0.020 mmol), 4-dimethylaminopyridine (dmap; 2.5 mg, 0.020 mmol), and C_6D_6 (0.5 mL). The resonances due to [η^5-1,2,4-$(Me_3C)_3C_5H_2]_2$Th[(μ-S)$_2$CPh$_2$] (**18**) along with those of Ph_2C═N(*p*-tolyl) and unreacted **4** were observed by ^{1}H NMR spectroscopy (50% conversion based on **4**).

Preparation of [η^5-1,2,4-$(Me_3C)_3C_5H_2]_2$Th[N(*p*-tolyl)-C(SSiMe_3)−S](Cl) (19). Me_3SiCl (1.0 mL) was added to a benzene (10 mL) solution of [η^5-1,2,4-$(Me_3C)_3C_5H_2]_2$Th[N(*p*-tolyl)C(S)-S] (**13**; 190 mg, 0.2 mmol) with stirring at room temperature. After this mixture was stirred overnight at 65 °C, the solution was filtered. The volume of the filtrate was reduced to 2 mL, and colorless crystals **19** were isolated from the mixture after this solution stood at room temperature for 3 days. Yield: 148 mg (75%). Mp: 108−110 °C (dec.). ^{1}H NMR (C_6D_6): δ 7.34 (d, J = 8.0 Hz, 2H, aryl), 7.03 (d, J = 8.0 Hz, 2H, aryl), 6.75 (d, J = 2.8 Hz, 2H, ring C*H*),

6.23 (d, J = 2.8 Hz, 2H, ring CH), 2.09 (s, 3H, tolylCH_3), 1.64 (s, 18H, $(CH_3)_3$C), 1.52 (s, 18H, $(CH_3)_3$C), 1.44 (s, 18H, $(CH_3)_3$C), 0.48 (s, 9H, $(CH_3)_3$Si). ^{13}C{^{1}H} NMR (C_6D_6): δ 187.0, 146.7, 146.0, 144.2, 143.2, 135.2, 128.8, 125.7, 121.3, 113.2, 35.2, 35.1, 34.9, 34.4, 33.9, 32.5, 20.7, 1.7. IR (KBr, cm^{-1}): ν 2961 (s), 1604 (m), 1439 (m), 1358 (m), 1260 (s), 1089 (s), 1017 (s), 798 (s). Anal. Calcd for $C_{45}H_{74}NClS_2SiTh$: C, 54.66; H, 7.54; N, 1.42. Found: C, 54.62; H, 7.61; N, 1.45.

Preparation of [η^5-1,2,4-$(Me_3C)_3C_5H_2$]$_2$Th[N(p-tolyl)C{N(Ph)($SiMe_3$)}−S](Cl) (20). Me_3SiCl (1.0 mL) was added to a benzene (10 mL) solution of [η^5-1,2,4-$(Me_3C)_3C_5H_2$]$_2$Th[N(p-tolyl)C(NPh)−S] (**14**; 190 mg, 0.2 mmol) with stirring at room temperature. After this mixture was stirred overnight at 65 °C, the solution was filtered. The volume of the filtrate was reduced to 1 mL, and colorless microcrystals **20** were isolated from the mixture after this solution stood at room temperature for 2 days. Yield: 172 mg (82%). Mp: 168−170 °C (dec.). ^{1}H NMR (C_6D_6): δ 6.77 (m, 6H, aryl), 6.64 (m, 1H, aryl), 6.50 (m, 4H, aryl and ring CH), 6.21 (d, J = 2.8 Hz, 2H, ring CH), 1.96 (s, 3H, tolylCH_3), 1.68 (s, 18H, $(CH_3)_3$C), 1.53 (s, 36H, $(CH_3)_3$C), 0.42 (s, 9H, $(CH_3)_3$Si). ^{13}C{^{1}H} NMR (C_6D_6): δ 178.7, 148.4, 145.8, 142.9, 140.2, 134.9, 132.4, 130.2, 129.1, 126.9, 125.4, 123.2, 122.4, 112.2, 35.2, 35.1, 35.0, 34.7, 34.0, 32.8, 20.6, 2.80. IR (KBr, cm^{-1}): ν 2961 (s), 1591 (s), 1460 (s), 1357 (s), 1259 (s), 1091 (s), 1016 (s), 798 (s). Anal. Calcd for $C_{51}H_{79}N_2ClSSiTh$: C, 58.46; H, 7.60; N, 3.38. Found: C, 58.42; H, 7.71; N, 3.35.

X-ray Crystallography. Single-crystal X-ray diffraction measurements were carried out on a Bruker Smart APEX II CCD diffractometer at 150(2) K using graphite monochromated Mo Kα radiation (λ = 0.71070 Å). An empirical absorption correction was applied using the SADABS program.[32] All structures were solved by direct methods and refined by full-matrix least-squares on F^2 using the SHELXL-97 program package.[33] All of the hydrogen atoms were geometrically fixed using the riding model. The crystal data and experimental data for **6**, **7**, **10**−**14**, **16**, **17**, and **19** are summarized in the Supporting Information. Selected bond lengths and angles are listed in Table 1.

Computational Methods. All calculations were carried out with the Gaussian 09 program (G09),[34] employing the Becke-3-Lee−Yang−Parr (B3LYP) method with standard 6-31G(d) basis set for C, H, O, N, and S elements and Stuttgart RLC ECP from EMSL basis set exahange (https://bse.pnl.gov/bse/portal) for Th element,[35] to fully optimize the geometries of reactants, complexes, transition state, intermediates, and product structures. The self-consistent reaction field (SCRF) polarizable continuum model (PCM) with default radii in G09 was also used to mimic experimental toluene-solvent conditions (dielectric constant ε = 2.379). All resultant stationary points were subsequently characterized by vibrational analyses, from which their respective zero-point (vibrational) energies (ZPE) were extracted and used in the relative energy determinations, in addition to ensuring that the reactant, complex, intermediate, product, and transition state structures resided at minima and first order saddle points, respectively, on their potential energy hypersurfaces.

■ ASSOCIATED CONTENT

Supporting Information. Complete list of authors for ref 34. Crystal parameters for compounds **6**, **7**, **10**−**14**, **16**, **17**, and **19**. ORTEP diagrams of **11**, **14**, and **16**. Cartesian coordinates of all stationary points optimized at the B3LYP/genecp level and imaginary frequencies of transition states. ^{1}H and ^{13}C NMR spectra of new compounds. X-ray crystallographic data, in CIF format, for compounds **6**, **7**, **10**−**14**, **16**, **17**, and **19**. This material is available free of charge via the Internet at http://pubs.acs.org.

■ AUTHOR INFORMATION

Corresponding Author

gzi@bnu.edu.cn; dcfang@bnu.edu.cn; mwalter@tu-bs.de

■ ACKNOWLEDGMENT

This work was supported by the National Natural Science Foundation of China (Grant nos. 20972018, 21074013, 21073016), the Program for New Century Excellent Talents in University (NCET-10-0253), the Fundamental Research Funds for the Central Universities (China), and the Deutsche Forschungsgemeinschaft (DFG) through the Emmy-Noether program (WA 2513/2-1). We thank Dr. Xuebin Deng for his help with the crystallography, and Professor Richard A. Andersen for helpful discussions.

■ REFERENCES

(1) For selected recent reviews, see: (a) Ephritikhine, M. *Dalton Trans.* **2006**, 2501–2516. (b) Szabo, Z.; Toraishi, T.; Vallet, V.; Grenthe, I. *Coord. Chem. Rev.* **2006**, *250*, 784–815. (c) Van Horn, J. D.; Huang, H. *Coord. Chem. Rev.* **2006**, *250*, 765–775. (d) Sessler, J. L.; Melfi, P. J.; Pantos, D. G. *Coord. Chem. Rev.* **2006**, *250*, 816–843. (e) Barnea, E.; Eisen, M. S. *Coord. Chem. Rev.* **2006**, *250*, 855–899. (f) Fox, A. R.; Bart, S. C.; Meyer, K.; Cummins, C. C. *Nature* **2008**, *455*, 341–349. (g) Andrea, T.; Eisen, M. S. *Chem. Soc. Rev.* **2008**, *37*, 550–567. (h) Graves, C. R.; Kiplinger, J. L. *Chem. Commun.* **2009**, 3831–3853. (i) Arnold, P. L.; Love, J. B.; Patel, D. *Coord. Chem. Rev.* **2009**, *253*, 1973–1978. (j) Hayton, T. W. *Dalton Trans.* **2010**, *39*, 1145–1158. (k) Fortier, S.; Hayton, T. W. *Coord. Chem. Rev.* **2010**, *254*, 197–214. (l) Arnold, P. L. *Chem. Commun.* **2011**, DOI: 10.1039/c1cc10834d.

(2) For selected papers on uranium nonmetallocenes containing terminal oxo groups, see: (a) Andersen, R. A. *Inorg. Chem.* **1979**, *18*, 1507–1509. (b) Docrat, T. I.; Mosselmans, J. F. W.; Charnock, J. M.; Whiteley, M. W.; Collison, D.; Livens, F. R.; Jones, C.; Edmiston, M. J. *Inorg. Chem.* **1999**, *38*, 1879–1882. (c) Duval, P. B.; Burns, C. J.; Buschmann, W. E.; Clark, D. L.; Morris, D. E.; Scott, B. L. *Inorg. Chem.* **2001**, *40*, 5491–5496. (d) Duval, P. B.; Burns, C. J.; Clark, D. L.; Morris, D. E.; Scott, B. L.; Thompson, J. D.; Werkema, E. L.; Jia, L.; Andersen, R. A. *Angew. Chem., Int. Ed.* **2001**, *40*, 3358–3361. (e) Roussel, P.; Boaretto, R.; Kingsley, A. J.; Alcock, N. W.; Scott, P. *J. Chem. Soc., Dalton Trans.* **2002**, 1423–1428. (f) Berthet, J.-C.; Nierlich, M.; Ephritikhine, M. *Angew. Chem., Int. Ed.* **2003**, *42*, 1952–1954. (g) Burdet, F.; Pecaut, J.; Mazzanti, M. *J. Am. Chem. Soc.* **2006**, *128*, 16512–16513. (h) Berthet, J.-C.; Siffredi, G.; Thuery, P.; Ephritikhine, M. *Chem. Commun.* **2006**, 3184–3186. (i) Natrajan, L.; Burdet, F.; Pecaut, J.; Mazzanti, M. *J. Am. Chem. Soc.* **2006**, *128*, 7152–7153. (j) Hayton, T. W.; Boncella, J. M.; Scott, B. L.; Batista, E. R. *J. Am. Chem. Soc.* **2006**, *128*, 12622–12623. (k) Hayton, T. W.; Wu, G. *J. Am. Chem. Soc.* **2008**, *130*, 2005–2014. (l) Arnold, P. L.; Patel, D.; Wilson, C.; Love, J. B. *Nature* **2008**, *451*, 315–317. (m) Hayton, T. W.; Wu, G. *Inorg. Chem.* **2008**, *47*, 7415–7423. (n) Bart, S. C.; Anthon, C.; Heinemann, F. W.; Bill, E.; Edelstein, N. M.; Meyer, K. *J. Am. Chem. Soc.* **2008**, *130*, 12536–12546. (o) Nocton, G.; Horeglad, P.; Pecaut, J.; Mazzanti, M. *J. Am. Chem. Soc.* **2008**, *130*, 16633–16645. (p) Hayton, T. W.; Wu, G. *Inorg. Chem.* **2009**, *48*, 3065–3072. (q) Berthet, J.-C.; Siffredi, G.; Thuery, P.; Ephritikhine, M. *Dalton Trans.* **2009**, 3478–3494. (r) Cantat, T.; Graves, C. R.; Scott, B. L.; Kiplinger, J. L. *Angew. Chem., Int. Ed.* **2009**, *48*, 3681–3684. (s) Horeglad, P.; Nocton, G.; Filinchuk, Y.; Pécaut, J.; Mazzanti, M. *Chem. Commun.* **2009**, 1843–1845. (t) Fortier, S.; Wu, G.; Hayton, T. W. *J. Am. Chem. Soc.* **2010**, *132*, 6888–6889. (u) Kraft, S. J.; Walensky, J.; Franwick, P. E.; Hall, M. B.; Bart, S. C. *Inorg. Chem.* **2010**, *49*, 7620–7622. (v) Brow, J. L.; Wu, G.; Hayton, T. W. *J. Am. Chem. Soc.* **2010**, *132*, 7248–7249. (w) Tourneux, J.-C.; Berthet, J.-C.; Cantat, T.; Thuéry, P.; Mézailles, N.; Ephritikhine, M. *J. Am. Chem. Soc.* **2011**, *133*, 6162–6165. (x) Schnaars, D. D.; Wu, G.; Hayton, T. W. *Inorg. Chem.* **2011**, *50*, 4695–4697. (y) Brown, J. L.; Mokhtarzadeh, C. C.; Lever, J. M.; Wu, G.; Hayton, T. W. *Inorg. Chem.* **2011**, *50*, 5105–5112.

(3) For selected papers about uranium metallocenes containing terminal oxo groups, see: (a) Villiers, C.; Adam, R.; Ephritikhine, M. *Chem. Commun.* **1992**, 1555–1556. (b) Arney, D. S. J.; Burns, C. J. *J. Am.*

Chem. Soc. **1993**, *115*, 9840–9841. (c) Arney, D. S. J.; Burns, C. J. *J. Am. Chem. Soc.* **1995**, *117*, 9448–9460. (d) Evans, W. J.; Kozimor, S. A.; Ziller, J. W. *Polyhedron* **2004**, *23*, 2689–2694. (e) Zi, G.; Jia, L.; Werkema, E. L.; Walter, M. D.; Gottfriedsen, J. P.; Andersen, R. A. *Organometallics* **2005**, *24*, 4251–4262.

(4) Ventelon, L.; Lescop, C.; Arliguie, T.; Leverd, P. C.; Lance, M.; Nierlich, M.; Ephritikhine, M. *Chem. Commun.* **1999**, 659–660.

(5) Morss, L. R., Edelstein, N. M., Fuger, J., Katz, J. J., Eds. *The Chemistry of the Actinide and Transactinide Elements*, 3rd ed.; Springer: Dordrecht, 2006; Vols. 1−5.

(6) Hutchings, G. J.; Heneghan, C. S.; Hudson, I. D.; Taylor, S. H. *Nature* **1996**, *384*, 341–343.

(7) *Gmelin Handbuch der Anorganischen Chemie, Thorium, Ergänzungsband Teil C1*; Springer-Verlag: Berlin, 1978.

(8) For selected papers on oxo and sulfido group 4 metallocenes, see: (a) Polse, J. L.; Andersen, R. A.; Bergman, R. G. *J. Am. Chem. Soc.* **1995**, *117*, 5393–5394. (b) Carney, M. J.; Walsh, P. J.; Bergman, R. G. *J. Am. Chem. Soc.* **1990**, *112*, 6426–6428. (c) Howard, W. A.; Parkin, G. *J. Am. Chem. Soc.* **1994**, *116*, 606–615. (d) Howard, W. A.; Trnka, T. M.; Waters, M.; Parkin, G. *J. Organomet. Chem.* **1997**, *528*, 95–121. (e) Tainturier, G.; Fahim, M.; Trouvé-Bellan, G.; Gautheron, B. *J. Organomet. Chem.* **1989**, *376*, 321–332. (f) Sweeney, Z. K.; Polse, J. L.; Andersen, R. A.; Bergman, R. G. *J. Am. Chem. Soc.* **1998**, *120*, 7825–7834.

(9) Parkin, G. *Prog. Inorg. Chem.* **1998**, *47*, 1–165.

(10) Selected recent papers about the bonding of organoactinide complexes, see: (a) Cantat, T.; Graves, C. R.; Jantunen, K. C.; Burns, C. J.; Scott, B. L.; Schelter, E. J.; Morris, D. E.; Hay, P. J.; Kiplinger, J. L. *J. Am. Chem. Soc.* **2008**, *130*, 17537–17551. (b) Barros, N.; Maynau, D.; Maron, L.; Eisenstein, O.; Zi, G.; Andersen, R. A. *Organometallics* **2007**, *26*, 5059–5065. (c) Yahia, A.; Maron, L. *Organometallics* **2009**, *28*, 672–679.

(11) Lukens, W. W., Jr.; Beshouri, S. M.; Blosch, L. L.; Andersen, R. A. *J. Am. Chem. Soc.* **1996**, *118*, 901–902.

(12) For the ionic radius of thorium (Th^{4+} = 1.08 Å) and uranium (U^{4+} = 1.03 Å), see:Cotton, F. A.; Wilkinson, G.; Murillo, C. A.; Bochmann, M. *Advanced Inorganic Chemistry*, 6th ed.; John Wiley & Sons: New York, 1999; p 1131.

(13) 5f orbitals play a key role in the bonding in actinide complexes, which leads to a very polarized M═E bond, whereas this does not occur for a group 4 metal complex.[10c] For example, the M═O is a single bond with an electrostatic interaction for actinide metals (i.e., $M^{+}-O^{-}$), while it is a double bond for group 4 metals.[10b,c]

(14) Bagnall, K. W. *The Actinide Elements*; Elsevier: Amsterdam, 1972.

(15) Nugent, W. A.; Mayer, J. M. *Metal Ligand Multiple Bonds*; Wiley-Interscience: New York, 1988.

(16) Guymont, M.; Livage, J.; Mazières, C. *Bull. Soc. Fr. Mineral. Cristallogr.* **1973**, *96*, 161–165.

(17) Haskel, A.; Straub, T.; Eisen, M. S. *Organometallics* **1996**, *15*, 3773–3775.

(18) Berg, J. M.; Clark, D. L.; Huffman, J. C.; Morris, D. E.; Sattelberger, A. P.; Streib, W. E.; Van Der Sluys, W. G.; Watkin, J. G. *J. Am. Chem. Soc.* **1992**, *114*, 10811–10821.

(19) Clark, D. L.; Watkin, J. G. *Inorg. Chem.* **1993**, *32*, 1766–1772.

(20) Lam, O. P.; Heinemann, F. W.; Meyer, K. *Chem. Sci.* **2011**, *2*, 1538−1547.

(21) Shein, K. I.; Shein, I. R.; Medvedeva, N. I.; Bamburov, V. G.; Ivanovskii, A. L. *Dokl. Phys. Chem.* **2006**, *409*, 198–201.

(22) Wrobleski, D. A.; Cromer, D. T.; Ortiz, J. V.; Rauchfuss, T. B.; Ryan, R. R.; Sattelberger, A. P. *J. Am. Chem. Soc.* **1986**, *108*, 174–175.

(23) Eastman, E. D.; Brewer, L.; Bromley, L. R. A.; Gilles, P. W.; Lofgren, N. L. *J. Am. Chem. Soc.* **1950**, *72*, 4019–4023.

(24) Shannon, R. D. *Acta Crystallogr., Sect. A* **1976**, *32*, 751–767.

(25) Zachariasen, W. H. *Acta Crystallogr.* **1949**, *2*, 291–296.

(26) This term has been used by Evans and his co-workers to describe their alternating nitride and azide bridged uranium clusters $[(C_5Me_4R)_2U(\mu\text{-}N)U(\mu\text{-}N_3)(C_5Me_4R)_2]_4$ (R = H, Me); for details, see: Evans, W. J.; Kozimor, S. A.; Ziller, J. W. *Science* **2005**, *309*, 1835–1838.

(27) Blake, P. C.; Lappert, M. F.; Taylor, R. G.; Atwood, J. L.; Hunter, W. E.; Zhang, H. *J. Chem. Soc., Dalton Trans.* **1995**, 3335–3341.

(28) Weber, F.; Sitzmann, H.; Schultz, M.; Sofield, C. D.; Andersen, R. A. *Organometallics* **2002**, *21*, 3139–3146.

(29) Edwards, P. G.; Weydert, M.; Petrie, M. A.; Andersen, R. A. *J. Alloys Compd.* **1994**, *213/214*, 11–14.

(30) Zhang, X.; Jiang, X.; Zhang, K.; Mao, L.; Luo, J.; Chi, C.; Chan, H. S. O.; Wu, J. *J. Org. Chem.* **2010**, *75*, 8069–8077.

(31) Jamir, L.; Ali, A. R.; Ghosh, H.; Chipem, F. A. S.; Patel, B. K. *Org. Biomol. Chem.* **2010**, *8*, 1674–1678.

(32) Sheldrick, G. M. *SADABS, Program for Empirical Absorption Correction of Area Detector Data*; University of Göttingen: Göttingen, Germany, 1996.

(33) Sheldrick, G. M. *SHELXL-97, Program for the Refinement of Crystal Structure from Diffraction Data*; University of Göttingen: Göttingen, Germany, 1997.

(34) Frisch, M. J.; et al. *Gaussian 09*, revision A.02; Gaussian, Inc.: Wallingford, CT, 2009.

(35) Kuechle, W.; Dolg, M.; Stoll, H.; Preuss, H. *Mol. Phys.* **1991**, *74*, 1245–1263.